Chemical Engineering Research and Design 214 (2025) 234–250

Contents lists available at ScienceDirect

Chemical Engineering Research and Design

journal homepage: www.elsevier.com/locate/cherd

Effect of solid particles on the hydrodynamics of vertical upward gas–liquid two-phase flow: Pressure drop analysis

Ronaldo Luís Höhn, Abderraouf Arabi, Sylvana Verónica Varela Ballesta, Paolo Juan Sassi, Jordi Pallarès, Youssef Stiriba *

Departament d'Enginyeria Mecànica, Universitat Rovira i Virgili, Av. Països Catalans 26, Tarragona, 43007, Catalonia, Spain

ARTICLE INFO

Keywords:
Gas–liquid two-phase flow
Gas–liquid–solid three-phase flow
Vertical upward flow
Pressure drop

ABSTRACT

Correct prediction of frictional pressure drop is crucial to designing and maintaining two- and three-phase flow systems. This study investigated experimentally the total and frictional pressure drop for gas–liquid and gas–liquid–solid flows with polypropylene (pellets) particles less dense than water, similar to hydrate particles encountered in offshore gas and oil production, in vertical co-current upward flow using a 30 mm ID pipe. The influence of the mixture Froude number (Fr_m) on the Chisholm coefficient is reported and explained by its noticeable effect on flow structure shape, observed with a high-speed camera. A new correlation is proposed based on two-phase experimental data. Twenty-seven existing correlations and the proposed one were assessed against existing literature data. The assessment of the new correlation with the database collected from the literature demonstrates its potential to be applied in a wide range of conditions for two-phase vertical upward flows. Additionally, the proposed model was also extended to the three-phase flow by considering the gas–liquid–solid three-phase flow as a gas-slurry two-phase flow. The average absolute relative error for the solid particle concentrations investigated was found to be less than 30%.

1. Introduction

Two-phase gas–liquid flow in pipelines is present in numerous industrial processes, from oil and gas transportation (Tarahomi et al., 2023; Shibata et al., 2023; Bouderbal et al., 2024) to nuclear power plants (Ryan et al., 2023; Zhang et al., 2024). A third solid phase frequently appears in a gas–liquid system, and in oil and gas production as sands (Fajemidupe et al., 2019; Zhang et al., 2020) or hydrate formation (Rosas et al., 2018; Cavalli et al., 2024). It is also frequent in wastewater treatment, the mining industry (Takano et al., 2023), and in many chemical reactions involving the suspension in a gas–liquid flow (Douek et al., 1997). In these processes, a reliable estimation of the pressure drop occurring in pipes and other equipment is fundamental to design the multiphase systems and to maintain the safety of the process in which these flows are present (Cai et al., 2022; Passoni et al., 2023). The total two-phase flow pressure drop is the sum of three components: gravitational, frictional, and accelerational, as shown in Eq. (1).

$$\left(\frac{dp}{dz}\right)_{Total} = \left(\frac{dp}{dz}\right)_{Grav.} + \left(\frac{dp}{dz}\right)_{Fric.} + \left(\frac{dp}{dz}\right)_{Accel.} \quad (1)$$

The term due to acceleration is generally neglected in the case of non-boiling two-phase flow (Saidj et al., 2018). The gravitational pressure drop is due to hydrostatic forces and is defined as:

$$\left(\frac{dp}{dz}\right)_{Grav.} = \rho_m g \sin\theta \quad (2)$$

where the mixture density, ρ_m, that is calculated as a weighted average of the liquid density, ρ_l, and the gas density, ρ_g, based on the liquid holdup, H_l:

$$\rho_m = \rho_l H_l + \rho_g (1 - H_l) \quad (3)$$

Among these three components, the frictional pressure drop is the most challenging to estimate due to its dependence on factors such as pipe inclination, flow pattern, as well as geometrical and fluid properties (Ghajar and Bhagwat, 2014; Lu et al., 2018; Muzychka and Awad, 2010; Arabi et al., 2021; Abdulkadir et al., 2020). Through the years, several empirical models have been proposed to predict the frictional pressure drop. There are two main common approaches to calculate this term: the homogeneous and the separate models. In the first approach, the two-phase flow is assumed to be a one-mixture single phase with an average of properties and velocities and with no-slip conditions between the phases (Shoham, 2006). This method relies on calculating the averaged properties of the mixture flow, often focusing on the viscosity estimation. Thus, the frictional pressure drop

* Corresponding author.
E-mail address: youssef.stiriba@urv.cat (Y. Stiriba).

https://doi.org/10.1016/j.cherd.2024.12.022
Received 5 September 2024; Received in revised form 6 December 2024; Accepted 16 December 2024
Available online 20 December 2024

Nomenclature

Latin Letters

C	Chisholm parameter [–]
D	Pipe diameter [m]
d	Diameter
dz/dz	Pressure drop gradient [Pa m^{-1}]
f	Friction factor [–]
Fr	Froude number [–]
G	Mass flux [Kg $m^{-2}s^{-1}$]
g	Gravitational acceleration [m/s^2]
H	Holdup/Volumetric fraction [–]
J	Superficial velocity [m s^{-1}]
K	Physical property coefficient [–]
La	Laplace number [–]
P	Pressure [Pa]
Pc	Maximum package concentration [–]
Re	Reynolds number [–]
V	Velocity [m s^{-1}]
We	Weber number [–]
X	Lockhart–Martinelli parameter [–]
x	Mass quality [–]
Y	Physical property coefficient [–]
z	Axial coordinate [m]

Greek Letters

α	Void fraction [–]
β	Gas volumetric flow fraction [–]
μ	Dynamic viscosity [Pa s]
Φ^2	Two-phase friction multiplier [–]
ρ	Density [kg/m^3]
σ	Surface tension [N m^{-1}]
θ	Inclination angle [rad]

Subscripts

2ϕ	Two-phase
3ϕ	Three-phase
$Accel$	Accelerational
$Fric$	Frictional
go	Gas phase only
$Grav$	Gravitational
g	Gas phase
lo	Liquid phase only
l	Liquid phase
m	Mixture
s	Solid phase

is calculated with the same formula employed in single phase flow. Different existing models for this approach are summarized in Table 1.

The separated approach considers pressure drop as the sum of single-phase liquid, single-phase gas, and interfacial losses (Muzychka and Awad, 2010). This approach was first introduced by Lockhart and Martinelli (1949). The proposed correlation was originally developed for horizontal pipelines and assumes the principle of each phase flowing separately in a part of the cross-section area based on the hydraulic diameter concept. The authors proposed two-phase frictional multipliers, Φ_l^2 and Φ_g^2, which are given by Eqs. (14) and (15). Later, Chisholm (1973), and Müller-Steinhagen and Heck (1986), among others, employed an alternative formulation. Their multipliers Φ_{lo}^2 and Φ_{go}^2 are based on the phase mass flux and can be defined by the Eqs. (16) and (17).

$$\left(\frac{dp}{dz}\right)_{l(Fric)} = \Phi_l^2\left(\frac{dp}{dz}\right)_{l(Fric)} = \Phi_l^2\left(\frac{2}{D}f_l\rho_l J_l^2\right) \tag{14}$$

$$\left(\frac{dp}{dz}\right)_{g(Fric)} = \Phi_g^2\left(\frac{dp}{dz}\right)_{g(Fric)} = \Phi_g^2\left(\frac{2}{D}f_g\rho_g J_g^2\right) \tag{15}$$

$$\left(\frac{dp}{dz}\right)_{2\phi(Fric)} = \Phi_{lo}^2\left(\frac{dp}{dz}\right)_{lo(Fric)} = \Phi_{lo}^2\left(\frac{f_l G_{2\phi}^2}{2D\rho_g}\right) \tag{16}$$

$$\left(\frac{dp}{dz}\right)_{2\phi(Fric)} = \Phi_{go}^2\left(\frac{dp}{dz}\right)_{go(Fric)} = \Phi_{go}^2\left(\frac{f_g G_{2\phi}^2}{2D\rho_g}\right) \tag{17}$$

where the subscripts l and g represent the frictional pressure gradient for single-phase liquid or gas flow at superficial velocity of J_l or J_g, respectively. The subscripts lo and go denote the frictional pressure gradient when the flow rate of the single-phase liquid or gas is considered equivalent to the two-phase flow mixture mass flux G. The parameter D is the internal diameter of the pipe and f is the frictional factor.

Based on these two separate approaches, researchers have developed other models. The most commonly used models are summarized in Table 2. Possibly the most popular model is the one proposed by Chisholm (1967), which suggests a simple Equation (18), that is based on a parameter (C) related to the Lockhart and Martinelli parameter (X). However, despite the great number of experimental investigations, developed correlations, and assessment studies on two-phase flow frictional pressure drop carried out for more than seven decades, this topic is still under investigation, as shown by the number of works carried out this last decade (Capovilla et al., 2019; Ryan et al., 2023; Zhang et al., 2024; Saidj et al., 2018; Lu et al., 2018; Arabi et al., 2021; Al-Ruhaimani et al., 2016; Sassi et al., 2020a).

Recently, Lu et al. (2018) proposed a value of 25 for the constant C for two-phase gas–liquid vertical upward pipelines, while Ryan et al. (2023) suggested $C = 26$. However, a fixed constant might not be ideal for the wide range of experimental conditions in two-phase vertical upward flows. This difficulty is also due to the influence of several parameters on the frictional pressure drop, as mentioned above. In their analysis, Cai et al. (2022) showed that the majority of studies reported errors greater than 10%, with some reaching up to 80%. Thus, contributing to the advancement of the frictional pressure drop correlation is one of the motivations for this paper.

For gas–liquid–solid flows, previous works generally model the predictive parameters based on those of gas–liquid two-phase flow (Sadatomi et al., 1990), since the same flow regimes in two-phase flow also occur in three-phase gas–liquid–solid flows and the liquid phase often acts as the main carrier of the solid particles. Based on these assumptions, two-phase models can be adapted for three-phase flow by considering the mixture properties of the liquid–solid slurry instead of the liquid phase alone. This approach has been usually adopted for modeling the frictional pressure drop in three-phase flows (Sadatomi et al., 1990; Hatakeyama and Masuyama, 1995; Rahman et al., 2013; Sassi et al., 2020b).

Concerning the solid–liquid slurry physical properties, it is well known that introducing suspended particles to a fluid increases its apparent viscosity (Guazzelli and Pouliquen, 2018), influenced by factors such as solid concentration, particle shape, interparticle interactions, spatial arrangement, and the characteristics of the bulk flow field (Mueller et al., 2009). The increase in apparent viscosity in liquid phases with the presence of a solid particle was studied by Thomas (1965), who proposed a simple but effective equation for the calculation of the slurry viscosity (Eq. (45)). This equation was used to calculate the mixture viscosity between solid and liquid (slurry phase) for the three-phase flow cases of this study.

$$\mu_{sl} = \mu_l\left[1.0 + 25C_s^2 + 0.062\exp\left\{1.875C_s/\left(1 - 1.595C_s\right)\right\}\right] \tag{45}$$

Table 1
Homogeneous approach.

McAdams (1949)	$\frac{1}{\mu_{2\phi}} = \frac{x}{\mu_g} + \frac{1+x}{\mu_l}$	(4)
Cicchitti et al. (1960)	$\mu_{2\phi} = (1-x)\,\mu_l + x\mu_g$	(5)
Dukler et al. (1964)	$\mu_{2\phi} = \rho_{tp}\left(\frac{x\mu_g}{\rho_g} + \frac{(1-x)\mu_l}{\rho_l}\right)$	(6)
Beattie and Whalley (1982)	$\mu_{2\phi} = \mu_l\,(1-\beta)\,(1+2.5\beta) + \mu_g\beta$	(7)
Fourar and Bories (1995)	$\mu_{2\phi} = (1-\beta)\,\mu_l + \beta\mu_g + 2\sqrt{\beta\,(1-\beta)\,\mu_l\mu_g}$	(8)
Shannak (2008)	$\mu_{2\phi} = \frac{[\mu_g x + \mu_l(1-x)(\rho_g/\rho_l)]}{x^2+(1-x)^2(\rho_g/\rho_l)}$	(9)
Awad and Muzychka (2008)	$\mu_{2\phi} = \mu_l\,\frac{2\mu_l+\mu_g-2(\mu_l-\mu_g)x}{2\mu_l+\mu_g+(\mu_l-\mu_g)x}$ (Definition 1)	(10)
Awad and Muzychka (2008)	$\mu_{2\phi} = \mu_g\,\frac{2\mu_g+\mu_l-2(\mu_g-\mu_l)(1-x)}{2\mu_g+\mu_l+(\mu_g-\mu_l)(1-x)}$ (Definition 2)	(11)
Awad and Muzychka (2008)	$\mu_{2\phi} = \frac{1}{2}\left(\mu_l\,\frac{2\mu_l+\mu_g-2(\mu_l-\mu_g)x}{2\mu_l+\mu_g+(\mu_l-\mu_g)x} + \mu_g\,\frac{2\mu_g+\mu_l-2(\mu_g-\mu_l)(1-x)}{2\mu_g+\mu_l+(\mu_g-\mu_l)(1-x)}\right)$	(12)
Maher et al. (2020)	$\mu_{2\phi} = \left((1-x)\,\mu_l + x\mu_g\right)^{0.94}\left(\frac{1-x}{\mu_l} + \frac{x}{\mu_g}\right)^{0.06}$	(13)

Table 2
Separated approach for frictional pressure drop.

Chisholm (1967)	$\Phi_l^2 = 1 + \frac{C}{X} + \frac{1}{X^2}$	(18)
	$C = \begin{cases} 5 \text{ for } Re_{sg} < 2000 \text{ and } Re_{sl} < 2000 \\ 10 \text{ for } Re_{sg} < 2000 \text{ and } Re_{sl} \geq 2000 \\ 12 \text{ for } Re_{sg} \geq 2000 \text{ and } Re_{sl} < 2000 \\ 20 \text{ for } Re_{sg} \geq 2000 \text{ and } Re_{sl} \geq 2000 \end{cases}$	(19)
Chisholm (1973)	$\Phi_{lo}^2 = 1 + \left(Y^2-1\right)\left(B\,[x\,(1-x)]^{0.875} + x^{1.75}\right)$	(20)
	$Y = \sqrt{\frac{(\Delta P/\Delta z)_{go}}{(\Delta P/\Delta z)_{lo}}}$	(21)
	$\text{if} = 0 < Y < 9.5,\ B = \begin{cases} 55/G_{2\phi}^2 \text{ if } G_{2\phi} \geq 1900\,\text{kg/m}^2\text{s} \\ 2400 \text{ if } 500 < G_{2\phi} < 1900\,\text{kg/m}^2\text{s} \\ 4.8 \text{ if } G_{2\phi} \leq 500 \end{cases}$	(22)
	$\text{if} = 9.5 < Y < 28,\ B = \begin{cases} 520/\left(YG_{2\phi}^2\right) \text{ if } G_{2\phi} \leq 600\,\text{kg/m}^2\text{s} \\ 21/Y \text{ if } G_{2\phi} > 600\,\text{kg/m}^2\text{s} \end{cases}$	(23)
	$\text{if} = Y > 28,\ B = 15000/\left(Y^2G_{2\phi}^{0.5}\right)$	(24)
Mandhane et al. (1977)	$X = \left(\frac{J_l}{J_g}\right)^{0.5}\left(\frac{\rho_l}{\rho_g}\right)^{0.375}\left(\frac{\mu_l}{\mu_g}\right)^{0.1}$	(25)
	$\Phi_G^2 = 0.6155X^{1.329} + 0.8041$	(26)
Müller-Steinhagen and Heck (1986)	$\Phi_{lo}^2 = Y^2x^3 + (1-x)^{1/3}\left[1 + 2x\left(Y^2-1\right)\right]$	(27)
Mishima and Hibiki (1996)	$C = 21\,[1 - exp(-0.319D)]$	(28)
Hwang and Kim (2006)	$La = \frac{[\sigma/(g(\rho_l-\rho_g))]^{0.5}}{D}$	(29)
	$C = 0.227Re_{lo}^{0.452}X^{-0.32}La^{-0.82}$	(30)
Zhang et al. (2010)	$C = 21\left[1 - exp(-0.674/La)\right]$	(31)
Wilson et al. (2003)	$\Phi_{lo}^2 = 12.82\,(1-x)^{1.8}\,X^{1.47}$	(32)
	$X = \left(\frac{1-x}{x}\right)^{0.9}\left(\frac{\rho_g}{\rho_l}\right)^{0.5}\left(\frac{\mu_l}{\mu_g}\right)^{0.1}$	(33)
Friedel (1979)	$K = \left(\frac{\rho_l}{\rho_g}\right)^{0.91}\left(\frac{\mu_l}{\mu_g}\right)^{0.19}\left(1 - \frac{\mu_g}{\mu_l}\right)^{0.7}$	(34)
	$Fr_{2\phi} = \frac{G_{2\phi}^2}{gD\rho_{2\phi}^2}$	(35)
	$We_{2\phi} = \frac{G_{2\phi}^2}{\sigma\rho_{2\phi}}$	(36)
	$\Phi_{lo}^2 = (1-x)^2 + x^2\frac{\rho_l f_{go}}{\rho_g f_{lo}} + \frac{3.24x^{0.78}(1-x)^{0.3224}K}{Fr_{2\phi}^{0.045}We_{2\phi}^{0.035}}$	(37)
Lu et al. (2018)	$C = 25$	(38)
Wallis (2020)	$\Phi_l^2 = \left[1 + \left(\frac{1}{X^{2/3.5}}\right)\right]^{3.5}$	(39)
Sun and Mishima (2008)	$\Phi_l^2 = 1 + \frac{1.79\left(\frac{Re_{sg}}{Re_{sl}}\right)^{0.4}\left(\frac{1-x}{x}\right)^{0.5}}{X^{1.19}} + \frac{1}{X^2}$	(40)
Awad (2007)	$\Phi_l^2 = \left[1 + \left(\frac{1}{X^2}\right)^{0.307}\right]^{1/0.307}$	(41)
Saisorn and Wongwises (2008)	$\Phi_l^2 = 1 + \frac{6.627}{X^{0.761}}$	(42)
Ryan et al. (2023)	$C = 26$	(43)
Whalley (1996)	$C = \left(\frac{\rho_l}{\rho_g}\right)^{1/2} + \left(\frac{\rho_g}{\rho_l}\right)^{1/2}$	(44)

The slurry density might be calculated in a similar way to the mixture density (ρ_m) with Eq. (46):

$$\rho_{sl} = \rho_l(1-C_s) + \rho_s C_s \tag{46}$$

Hatate et al. (1986) studied the effect of the solid particle diameter and concentration on frictional pressure drop using two pipe diameters (15.5 and 25.9 mm ID) and glass spheres with a $\rho_s = 2520\,\text{kg/m}^3$

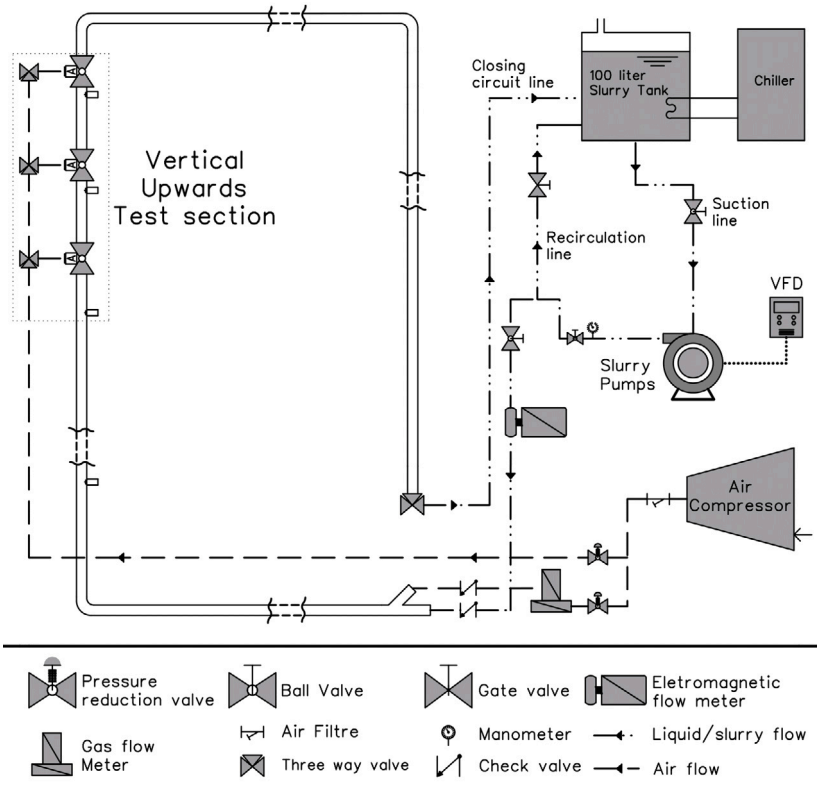

(a) Schematic of the experimental facility

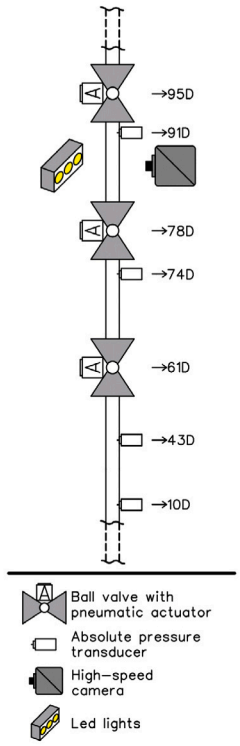

(b) Schematic of the vertical upward test section

Fig. 1. Experimental facility.

as the solid phase. In contrast to the particle diameter, the pressure drop was found to be strongly impacted by the solid concentration. The authors reported that the predictions of the modified Lockhart–Martinelli correlation diminish in the high range of gas superficial velocity investigated. In contrast, satisfactory results were achieved when using the model of Hughmark (1965), which considers the mean slurry velocity. Sakaguchi et al. (1993) studied the effect of aluminum ceramic particles (d_s = 2.57 mm and ρ_s = 2380 kg/m^3) on total, gravitational, and frictional pressure drops for slug flow. The authors observed that increasing the liquid flow rate and solid particles led to an increase in the three pressure drop terms. Additionally, an increase in gas superficial velocity reduced both total and gravitational pressure drops. Sakaguchi et al. (1993) found no significant effect of J_g on frictional pressure drop for the test conditions investigated. The authors also reported that the model of Sadatomi et al. (1990) accurately predicted the frictional pressure drop. Zhang et al. (2020) found lower values of the friction factor of the gas–oil–sand mixture compared to the gas–oil mixture.

More recently, Takano et al. (2023) used their generated database, as well as those of Takano et al. (2020, 2021), with glass beads (ρ_s = 2553 kg/m^3 and d_s = 4 mm) and resin balls (ρ_s = 1356 kg/m^3 and d_s = 6 mm) as solid particles, to assess the three-phase frictional pressure drop models of Sadatomi et al. (1990) and Hatakeyama and Masuyama (1995). Better performances were obtained with the model of Hatakeyama and Masuyama (1995). The authors proposed a model by assuming that solid particles are only present in the liquid phase and by neglecting the energy losses caused by the collision of the solid particles with the pipe wall. The proposed model gave a similar performance as the model of Hatakeyama and Masuyama (1995). Takano et al. (2023) explained that their model has the advantage of being purely theoretical and independent of empirical parameters. Previous studies typically used solid particles denser than water ($\rho_s/\rho_l > 1$). For particles less denser than water, there are only few works mainly for horizontal pipes such as those of Sassi et al. (2020b). Consequently, the extension of findings and outcomes of pressure drop to cases of three-phase flow when $\rho_s/\rho_l < 1$ is still questionable.

This study aims to improve the comprehension of the total and frictional pressure drop generated in vertical upward gas–liquid two-phase and gas–liquid–solid three-phase flows. A new experimental database of total and frictional pressure drops was generated using air, water, and solid particles less dense than water (ρ_s = 866 kg/m^3), similar to hydrate particles that form during the production of gas and oil in offshore, using a 30 mm ID pipe. These data enrich the existing database for pipe diameters greater than 10 mm where there is a lack in the literature according to Lu et al. (2018). Additionally, a new correlation is proposed based on the Lockhart–Martinelli approach for gas–liquid two-phase flow. The effect of solid concentration on total and frictional pressure drops is discussed, and the extension of the developed predictive correlation to gas–liquid–solid three-phase upward flows is also evaluated along with other literature models.

2. Test facility, measurement and evaluation methods

The experiments are performed in the low-pressure multiphase flow loop experimental facility at the department of mechanical engineering, University of Rovira i Vergili (Spain). The facility has been used to study volumetric fractions and frictional pressure drop in two- and three-phase flow studies in horizontal pipelines (Sassi et al., 2020a,b, 2022). Fig. 1 shows a simplified facility diagram of the experimental facility. The flow loop facility has 30 mm ID straight transparent acrylic pipes, and it was projected with horizontal, vertical upward, and vertical downward connected by 90° bends with a radius of curvature of 219.9 mm.

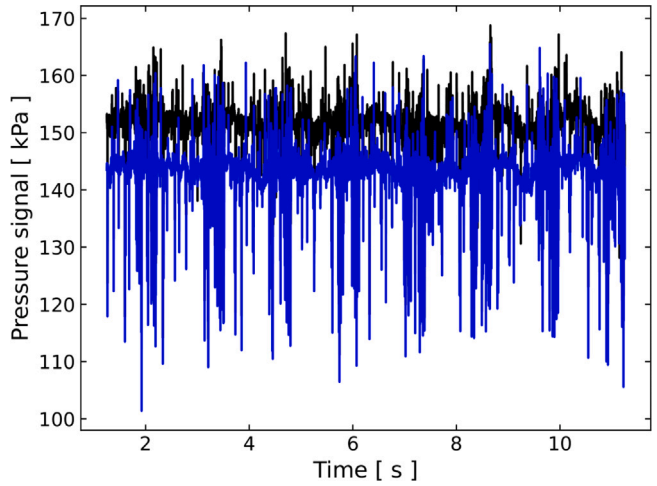

Fig. 2. Time series of pressure collected for slug flow pattern.

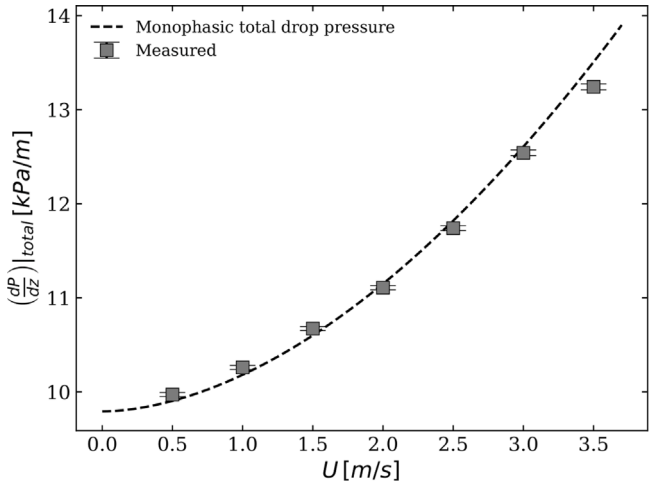

Fig. 3. Experimental single-phase total pressure drop comparison with the Darcy–Weisbach equation plus the gravitational pressure drop.

The liquid phase consisted of tap water, and the gas phase was compressed air previously filtered from the laboratory manifold. Polypropylene pellets were used as the solid phase, with diameters between 1 and 2 mm and a density of $\rho_s = 866$ kg/m^3 and a maximum packing density of $Pc = 0.585$. The solid particles were added to a 100-liter slurry tank, and the homogeneity of the slurry flow was controlled by an increase in the turbulence in the tank with a recirculation line controlled by a globe valve (see Fig. 1(a)). The selected solid concentrations (C_s= 5%, 10%, or 20%) were verified in the test section by trapping the water–solid slurry flow using a quick-closing valve system (see Fig. 1(b)). The same technique was used to verify the solid concentrations for each gas-slurry condition before the measurement of the pressure.

The gas and liquid/slurry phases were injected into the facility through a "Y" inlet junction at the horizontal test section. The superficial gas velocity is controlled by an Omega mass flowmeter controller with an accuracy of ±0.8%, where the gas phase enters at the upper part of the "Y" inlet junction and mixes with the liquid/slurry at the developing section (see Fig. 1(a)). The water/slurry phase was circulated using a 5.5 kW Weir AB80 centrifugal slurry pump through a suction line connected to the inlet junction. The flow rate was measured with an Isoil MS2500 electromagnetic flow meter with an accuracy of ±0.8%.

The vertical test sections were 35 diameters long, with a previous segment of 60 diameters and an addition of 17 diameters upstream section to minimize flow disruption (see Fig. 1(b)). Four Omega absolute pressure transducers with the accuracy value (compensated range) of ±0.3% measure the pressure signals. The transducers are distributed throughout the pipeline and have a range of 0 to 60 psi (0 to 4.13 bar). The total pressure drop was measured considering the two transducers' signals located at the highest lengths (74D and 91D) (see Fig. 1(b)). The signals are processed by a Keysight U2542 A USB data acquisition system, with a selected sampling rate of 4000 Hz to measure the pressure drop. Fig. 2 shows two examples of the pressure signals for the slug and churn flow patterns. The existence of important fluctuations is due to the flow of the two structures: liquid slug and elongated bubble. For each condition of solid concentration as well as liquid and gas superficial velocities, the measured total pressure drop is the average of 60 s for each signal value collected, and the total pressure drop is calculated from the difference between the two transducers.

An evaluation of the accuracy of the transducers was performed by measuring the monophasic flow pressure drop and comparing the results with the sum of the theoretical Darcy–Weisbach equation and the gravitational component, (see Fig. 3). Monophasic total drop pressure measures were performed regularly to check the conditions of the transducers. The average error of the monophasic total pressure drop measurements was 0.81%, and for the frictional pressure drop, it was 6.94%.

Table 3 summarizes the test conditions considered in this study. Pressure signals were measured for the cap-slug bubble, slug, churn, and dispersed-bubble flow patterns. A total of 66 two-phase cases were investigated with a liquid superficial velocity ranging from 0.75 m/s to 3.5 m/s and a gas superficial velocity range of 0.2 m/s to 7 m/s. For three-phase flow, a total of 114 cases were conducted. The temperature of the water and slurry mixture during the experiments ranged from 19 °C to 26 °C.

To support the development and the evaluation of the new frictional correlation, this study collected data from the literature on the frictional pressure drop of the two-phase vertical upward flow. These literature data include a different range of internal diameters, pipe lengths, superficial phase velocities, and air–water mixture. Table 4 summarizes these studies and the corresponding experimental conditions.

The data reported in Table 4 were compared with the predictions of the proposed developed correlation and the literature models presented in Tables 1 and 2. To evaluate the effectiveness of these correlations, two statistical parameters have been used to assess the results: Average percentage difference (*APD*) (Eq. (47)) and Average absolute percentage difference (*AAPD*) (Eq. (48)).

$$APD = \frac{1}{n}\sum_{k=1}^{n}\left[\frac{Cal. - Exp.}{Exp.}\right] \times 100 \tag{47}$$

$$AAPD = \frac{1}{n}\sum_{k=1}^{n}\left|\frac{Cal. - Exp.}{Exp.}\right| \times 100 \tag{48}$$

3. Results and discussion

In this section, the experimental two-phase data are initially presented in terms of total and frictional pressure drop, followed by a similar presentation of three-phase flow data. Additionally, the frictional pressure drop for two-phase flow is examined with the Lockhart–Martinelli analysis. Subsequently, a new correlation is proposed and explained. The proposed correlation, along with twenty-seven literature models, is evaluated using the collected literature data. Finally, the predictions of the existing models and the new correlation are compared to the experimental three-phase flow data.

Table 3
Test conditions.

Flow type	Solid concentration	Test conditions	J_l [m/s]	J_g [m/s]
2P	0%	66	0.75–3.5	0.2–7.0
3P-5%	5%	58	0.75–3.5	0.2–7.0
3P-10%	10%	26	0.75–3.0	0.2–7.0
3P-20%	20%	29	0.75–3.0	0.2–7.0

Table 4
Detail of the experimental conditions of the collected database.

Authors	D (m)	Length (L/D)	J_l (m/s)	J_g (m/s)	Liquid-phase	Gas-phase
Present study	0.03	74	0.75–3.5	0.2–7.0	Water	Air
Aggour (1978)	0.0117	139	0.315–10.59	0.07–88.5	Water	Air
Abdulkadir et al. (2021)	0.067	72.5	0.05–0.54	0.06–1.13	Silicone oil	Air
Lu et al. (2018)	0.0508	61.5	2.0–4.0	0.078–2.63	Water	Air
Saidj et al. (2018)	0.034	125	0.015–0.918	0.02–2.04	Water	Air
Sujumnong (1997)	0.01168	135	0.046–8.464	0.02–119.2	Water G1: 59% glycerine G2: 82% glycerine	Air
Tang et al. (2013)	0.0127	–	0.08–1.17	0.38–20	Water	Air
Shibata et al. (2023)	0.0527	485.5 51.2	1.5–2.5	1.1–7.7	Water	Air

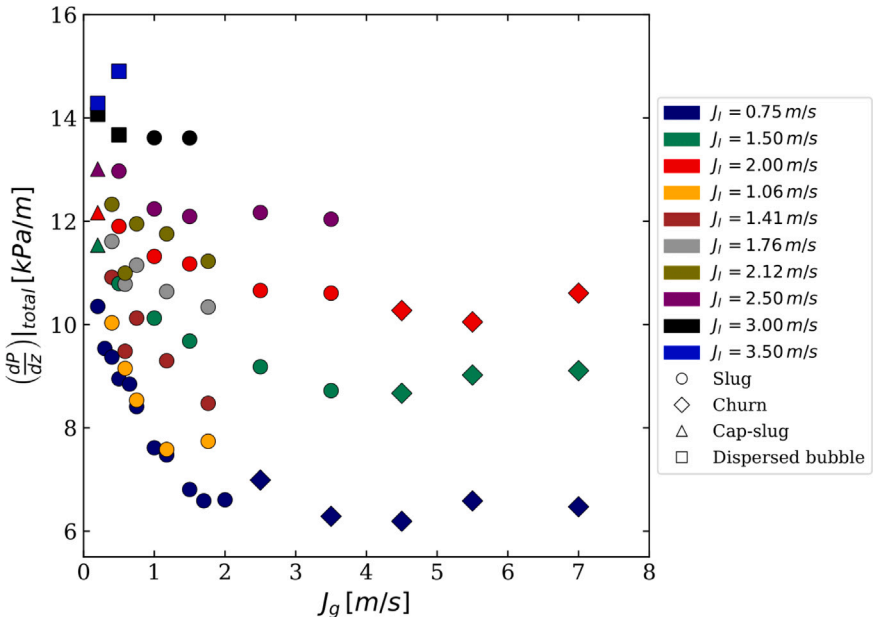

Fig. 4. Experimental two-phase total pressure drop as a function of the J_g for different values of J_l.

3.1. Total pressure drop for two-phase flow

The experimental total pressure drops for two-phase cases are plotted as a function of the superficial gas velocity for different superficial liquid velocities in Fig. 4. The expected reduction in the total pressure drops with the increase in superficial gas velocity was observed for each fixed J_l. For cases with J_l equal to 2.5, 2.0, and 1.5 m/s, the decrease in the values of the total pressure drop reaches a plateau, remains almost constant for the next few cases, and shows a tendency to increase slightly in the last points. This behavior occurs because the increase of the superficial gas velocity causes a natural decrease in the liquid holdup (H_l), which, consequently, reduces the mixture density of the two-phase flow and directly reduces the gravitational pressure drop component. The reduction of the total pressure drop with the increase of the superficial gas velocity has a limited effect and begins to reverse again when it reaches a relatively large value of the superficial gas velocity. When J_g attains this critical value, the frictional component drop pressure gains importance. The minimum value of the total pressure drop is frequently related to the transition from churn to annular flow pattern (Hewitt, 1985). However, a significant reduction in the values of the total pressure drop is also observed in the transition from slug to churn flows (Jayanti and Hewitt, 1992; Arabi et al., 2022; Owen, 1986). The minimum point of total pressure drop is related to the liquid flow rate (Owen, 1986), and the value of frictional pressure drop tends to increase abruptly in the early churn flow pattern, and it is reduced until it achieves the transition from churn to annular flow pattern.

The increase in the superficial liquid velocity leads to an increase of the total drop pressure, as mentioned by Sawai et al. (2004) and Saidj et al. (2018) among others. This is due to the natural increase of the liquid holdup with the increase in superficial liquid velocity (Shoham, 2006; Shibata et al., 2023), which raises the value of the gravitational component.

3.2. Frictional pressure drop for two-phase flow

The gravitational term can be subtracted from the total pressure drop to obtain the frictional pressure drop. This technique has been

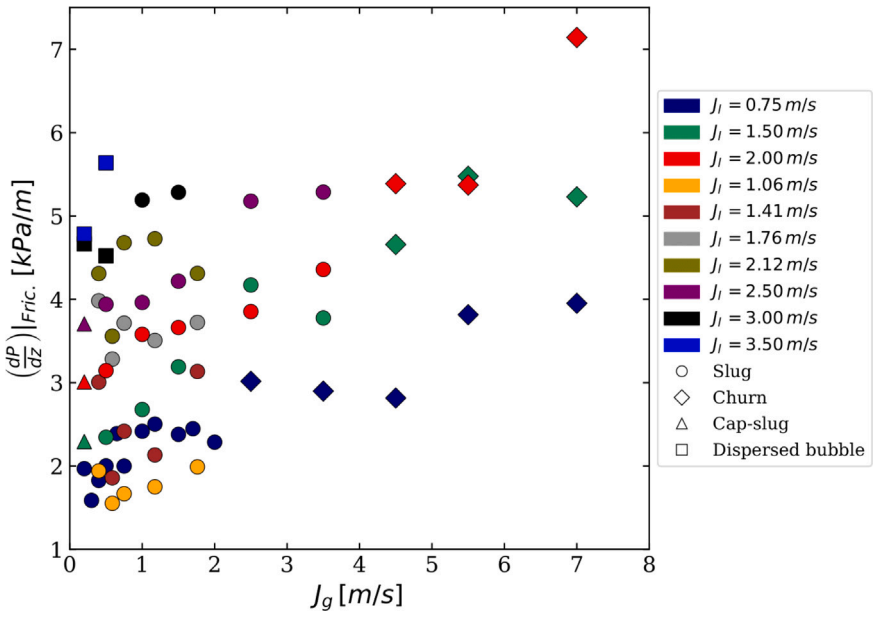

Fig. 5. Experimental two-phase frictional pressure drop as a function of the J_g for different values of J_l.

widely used in studies of two-phase flow (Shibata et al., 2023; Saidj et al., 2018; Lu et al., 2018) and three-phase flow (Hatate et al., 1986; Sakaguchi et al., 1993).

Fig. 5 shows the relationship between the two-phase vertical upward frictional pressure drop and the superficial gas velocity. As the superficial liquid and gas velocities increase, the frictional pressure drop also increases, as described by Shibata et al. (2023). It is known that the flow pattern can affect global parameters including the frictional pressure drop (Arabi et al., 2021; Abdulkadir et al., 2021). Fig. 5 shows that the transition from slug to churn flow coincides with a significant increase in frictional pressure drop. This can be explained by the high turbulence and discontinuous interfaces, which increase the shear stress in this flow regime (Sawai et al., 2004). Meanwhile, a relative stabilization of frictional pressure drop occurs at $J_l = 0.75$ m/s for the churn flow.

3.3. Total and frictional pressure drop for three-phase flow

The obtained total and frictional pressure drop as function of J_g for the three solid concentrations in the three-phase flow are shown in Fig. 6 for three different values of J_l. Note that the two-phase flow measurements were also displayed for comparison purposes.

A comparison between two-phase and three different solid concentrations of total pressure drop data shows that no visible impact of the presence of a solid is observed for the great majority of experimental measurement points. Concerning the effect of solid concentration on the frictional pressure drop, and considering the fact that the solid/liquid density ratio is relatively close to 1, which means that the gravitational pressure drop is not much influenced by the presence of solid phase, the independence of frictional pressure drop to solid concentration is expected. The obtained results show this behavior for the majority of points considered. Similar observations were reported for horizontal pipe (Sassi et al., 2020b). Besides, a deep observation shows that some experimental conditions exhibit a decrease of frictional pressure drop with increasing solid concentration, as shown in Fig. 6(b) for $J_l = 0.75$ and low J_g. While the opposite behavior occurs also for some conditions at higher values of J_g. These observations arise into the surface the complex nature of gas–liquid–solid three-phase flow.

From a theoretical point of view, the addition and increasing of solid concentration induce an increase of the slurry viscosity, and thus the frictional losses. Indeed and based on Equation 45, the viscosities for 5%, 10%, and 20% slurry are 1.13×10^{-3}, 1.32×10^{-3}, and 2.11×10^{-3} Pa.s, respectively, which are not negligible. However, the general tendency observed proves the occurrence of other complex phenomena that compensate the increment of slurry viscosity. As explained recently in Cavalli et al. (2024), the addition and increasing the solid concentration can induces both increasing and damping of liquid turbulence. Moreover, various phenomena of several scales are also present in gas–liquid–solid three-phase which impact on the hydrodynamic of the flow structures and the interface shapes. According to Douek et al. (1997), the solid concentration induces a direct impact on bubble coalescence. Indeed, the majority of experimental points of the present study has concerned slug flow which is governed by several slug parameters (slug length, elongated bubble length, slug translational velocity, slug liquid holdup and slug frequency). The solid particles impact directly the slug parameters (Rosas et al., 2018; Sassi et al., 2022), which in turn influences directly on the frictional pressure drop (Arabi et al., 2024). The difficulty to carry out local measurements for gas–liquid–solid three-phase makes it difficult to explain the physical phenomena occurring in this kind of multiphase flow, as reported recently by Cavalli et al. (2024).

3.4. Lockhart–Martinelli analysis

As mentioned in Section 1, the most common method for calculating the frictional pressure drop in separated flows, which is still being studied for cases with upward two-phase flow in vertical pipes (Shibata et al., 2023; Ryan et al., 2023; Lu et al., 2018). Fig. 7(a) displays the liquid two-phase flow multipliers (Φ_l) as function of the Lockhart and Martinelli parameters (X). The Chisholm constant (C) equal to 20 is plotted alongside with the measured and collected literature data. For most cases where $X < 0.5$, using a constant C of 20 provides a satisfactory approximation. After this critical value, a significant number of data points are not aligned with the $C = 20$ value.

In this study, different behaviors were observed related to the flow patterns, and the calculated fitted value of C was 36, as shown in Fig. 7(b). The dispersed bubble flow and most of the churn flow cases

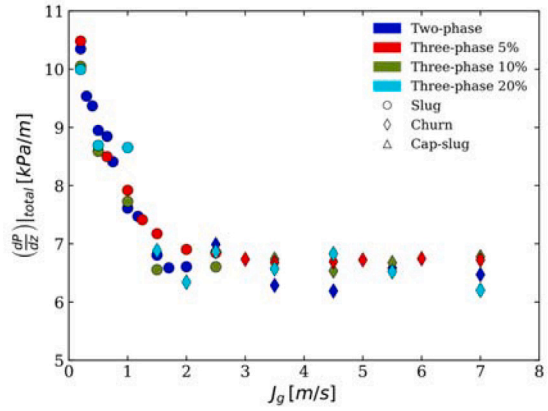

(a) Total drop pressure for $J_l = 0.75$ m/s

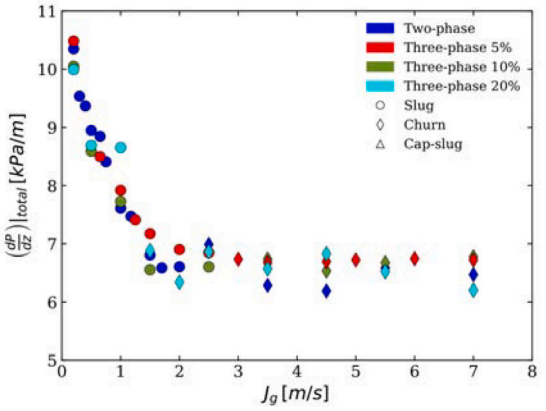

(b) Frictional drop pressure for $J_l = 0.75$ m/s

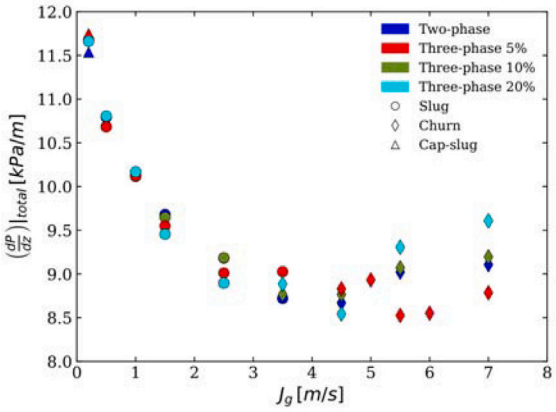

(c) Total drop pressure for $J_l = 1.50$ m/s

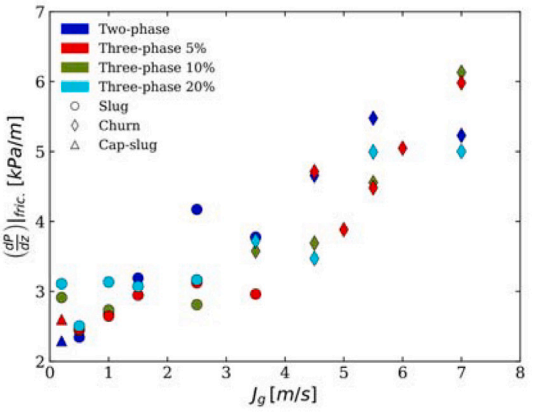

(d) Frictional drop pressure for $J_l = 1.50$ m/s

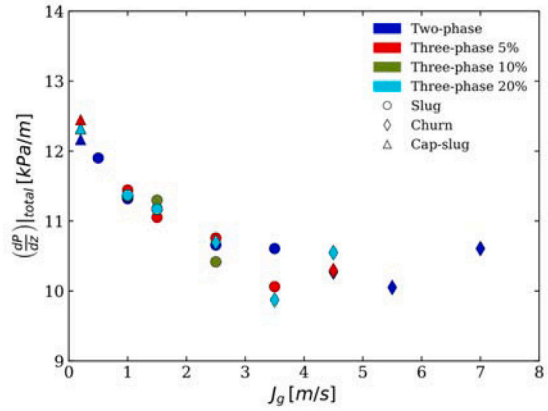

(e) Total drop pressure for $J_l = 2.00$ m/s

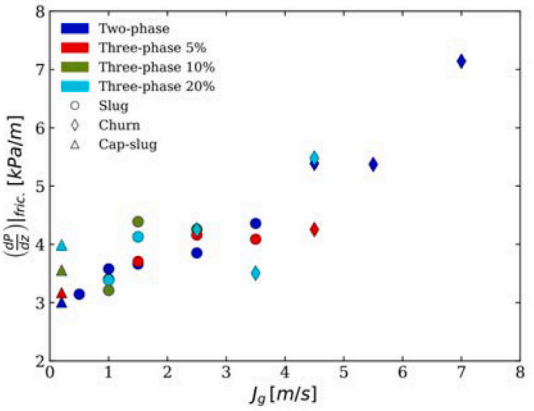

(f) Frictional drop pressure for $J_l = 2.00$ m/s

Fig. 6. Experimental total and frictional pressure drop as function of J_g: Three-phase Flow.

follow the constant equal to 20. However, other flow patterns show significantly higher values of C. As discussed in Section 1, some studies have investigated the optimal value for the constant C in vertical upward pipe flow. For example, Lu et al. (2018) found an optimal value of 25, while Ryan et al. (2023) proposed a value of 26. However, Dang et al. (2018) reported a fitting value of 100 for vertical upward flow, significantly larger than the other two studies. Additionally, Shibata et al. (2023) found different ideal values of C for different pipe lengths, with a C equals to 28 for a pipe length of 2.7 m and a C equals to 52 for a pipe length of 25.7 m. These variations in the constant C may indicate that the complexity of all possible flow scenarios for the two-phase upward flow might not be adjusted with a single value. Note that the obtained C value in the present study is in the range of the values reported in the literature.

3.5. New model for two-phase flow frictional pressure drop

Based on the observation that a single constant of C cannot predict all the data presented in Section 3.3, we investigated the influence of the Froude number (Fr_m), given by Eq. (49), on the values of C.

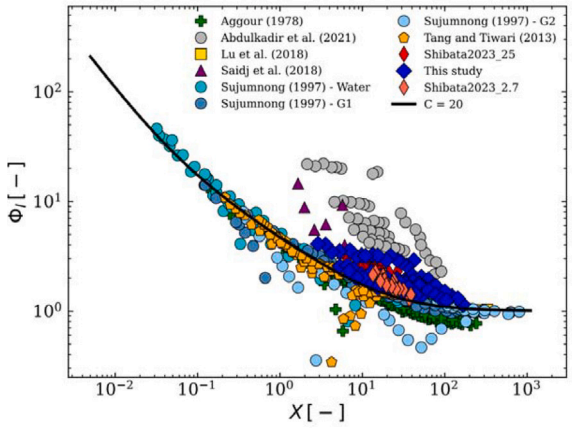

(a) Data collected from the literature

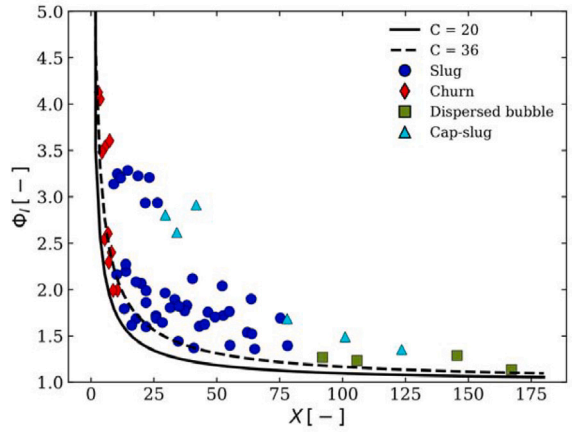

(b) Two-phase experimental data by flow patterns with the fitted $C = 36$

Fig. 7. Experimental data predicted by the Lockhart and Martinelli approach (Eq. (14)) for two-phase data and literature data.

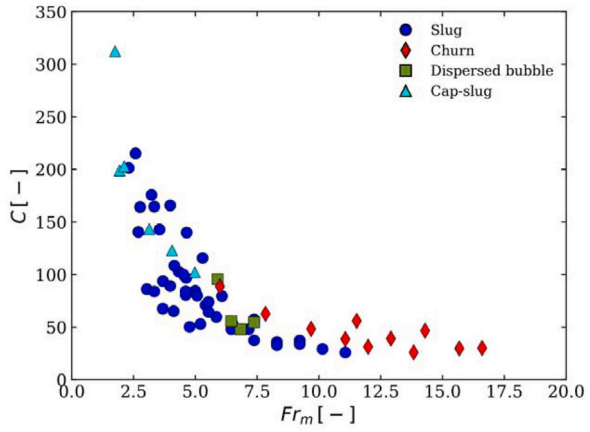

(a) Adjusted Chisholm constant for different Froude numbers and flow patterns

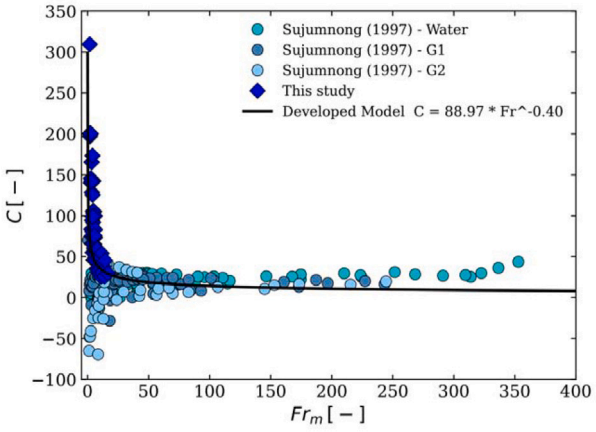

(b) Experimental and Sujumnong (1997) data with the developed correlation for $C*$

Fig. 8. Relation of the Froude number and the modified Chisholm constant C^* of the proposed model.

Fig. 8(a) shows this relationship with our results. It is clear that an increase in Fr_m induces a rapid decrease in C. The dimensionless Froude number relates opposing effects of gravity and inertia. This force competition impacts the dynamics and characteristics of the two-phase flows in vertical pipes (Maldonado et al., 2024). For $Fr_m \geq 8$, which corresponds approximately to the slug-to-churn flow transition, the Chisholm coefficient becomes essentially constant. The plot also shows the direct relationship between the flow regimes and the mixture Froude number. Indeed, lower and higher values correspond, respectively, to cap bubble and churn flows. While the slug flows are present in a great range of Fr_m.

$$Fr_m = \frac{V_m}{\sqrt{gD}} \sqrt{\frac{\rho_l}{\rho_l - \rho_g}} \tag{49}$$

By applying a power law fitting to our experimental data and data collected by Sujumnong (1997), a new empirical model for the Chisholm constant is proposed (see Fig. 8(b)):

$$C^* = 88.97\ Fr_m^{-0.4} \tag{50}$$

Considering Eq. (50), the new formula of the two-phase flow multiplier holds as:

$$\phi_l^2 = 1 + \frac{88.97\ Fr_m^{-0.4}}{X} + \frac{1}{X^2} \tag{51}$$

Note that the data from Sujumnong (1997) was used to expand the range of Fr_m data. This supporting data also includes water and 59% and 82% glycerine concentrations, identified as G1 and G2, respectively, in Fig. 8(b). The glycerine mixtures in G1 and G2 have significantly higher viscosities than water, and these two data reduce the influence of higher Froude numbers by lowering the exponent in the proposed equation. This aligns with the observed behavior of reduction in the slope of C^* as Fr_m increases, especially after the transition from slug to churn flow at approximately $Fr_m \geq 8$ (see Fig. 8(a)). The Sujumnong (1997) data add to the proposed equation different liquid viscosities, expand the range of mixture velocities (V_m), and includes data points from annular and high-speed churn flow patterns not achievable within the current experimental setup. It is interesting to note that the results of Sujumnong (1997) obtained with G1 and G2 exhibit points where $C < 0$. This means that the frictional pressure drop is less important than the addition of the liquid and gas pressure drop. Further experimental investigation has to be carried out to explain this behavior.

To understand and explain the direct influence of Fr_m on the frictional pressure drop, images of the flow were analyzed. The captured images of the slug flow for different values of the mixture Froude numbers are shown in Fig. 9. One can clearly see that as the Froude number increased, the number of dispersed bubbles carried by the liquid slugs also increased. This relatively large number of dispersed bubbles in the liquid phase causes deformations on the interface of the elongated bubble and, therefore, modifies the velocity, drag coefficient, and trajectory, Maldonado et al. (2023). Furthermore, the presence of dispersed bubbles increased in the regions close to the nose and the

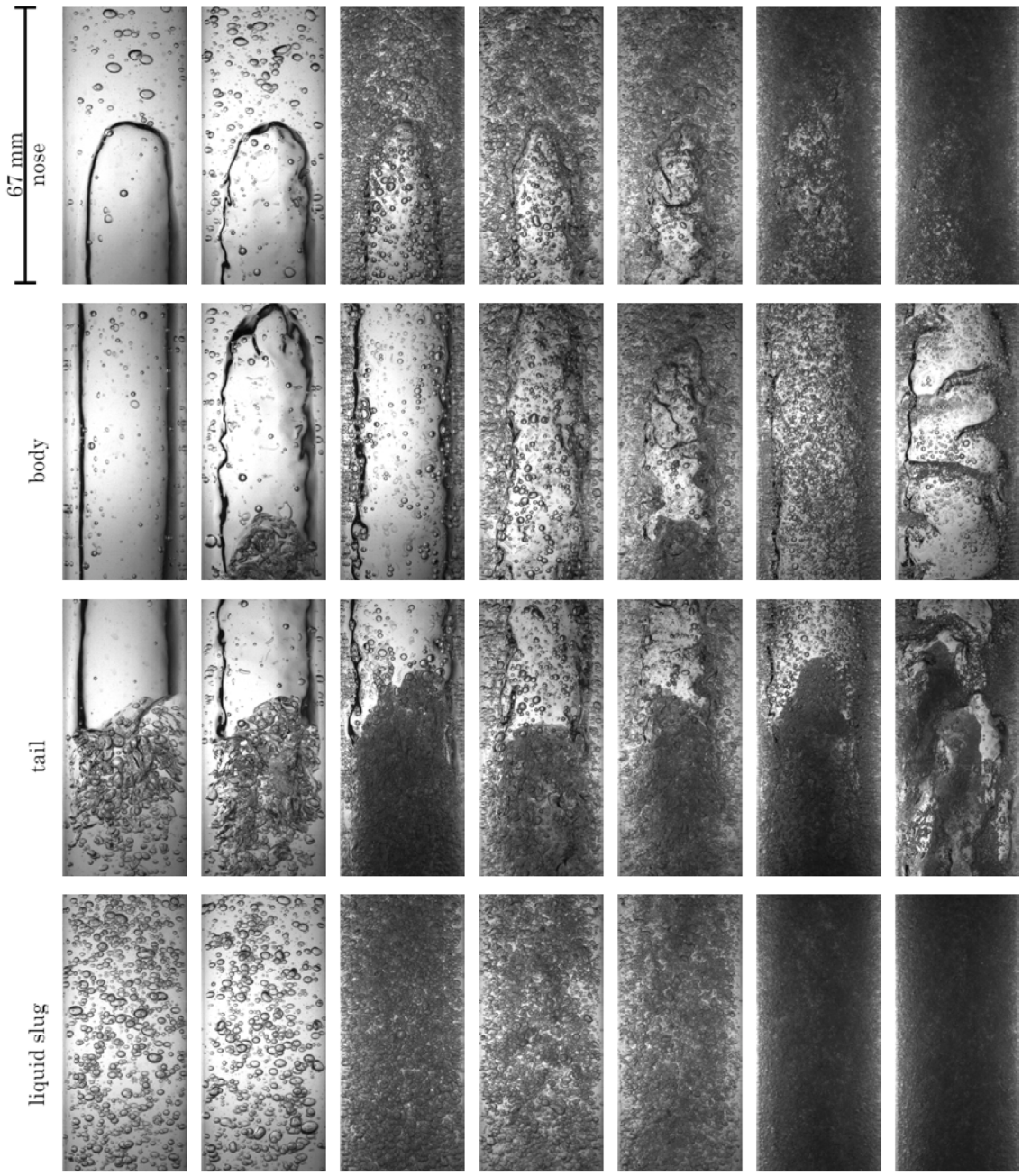

Fig. 9. Images of different elongated bubbles of two-phase flow at different Froude numbers.

tail of the elongated bubbles. The nose shape becomes sharper, and the shape of the tail passes from almost flat to highly unstable as the values of Fr_m gradually increase since the inertia in the liquid phase is the dominant effect and induces stronger turbulent fluctuations. The body of the elongated bubble is also affected at higher values of Fr_m. The interface becomes wavy and unstable, and the presence of dispersed bubbles becomes more pronounced in the annular liquid film. This complicates the detection of the elongated bubble tail/liquid slug nose interface. At Fr_m = 12.91, the dominant flow pattern corresponds to churn flow, and the equivalent observation for the slug pattern also applies, in which the instabilities on the elongated bubble contribute to the formation of this flow regime. These observations agree with those reported in the studies of Maldonado et al. (2024, 2023), who used wire-mesh sensors, and high-speed cameras to investigate the dispersed small bubbles and the Taylor bubble shape for different Froude numbers.

The same analysis was applied to the three-phase flow cases. Fig. 10 shows the influence of the increase in Fr_m in the flow structures for cases with 5% solid concentration. Similar flow behaviors observed in two-phase flow cases were also visualized for gas–liquid–solid flows. Solid particles dragged by the liquid flow are present near the bubble nose and the liquid film. Close near the bubble nose, the inertial effect leads to high velocity gradients, which promote liquid turbulence, and the nose becomes sharper and more distorted. The continuous increase in Fr_m leads to an increase in the dispersed bubbles and solid particles carried by the liquid/slurry phase toward the near wake region. For Fr_m > 4.15, the bubble tail becomes irregular, and the bubble dispersed in the liquid becomes smaller and nearly spherical. Additionally, the presence of solid particles may also modify the coalescence of the bubbles.

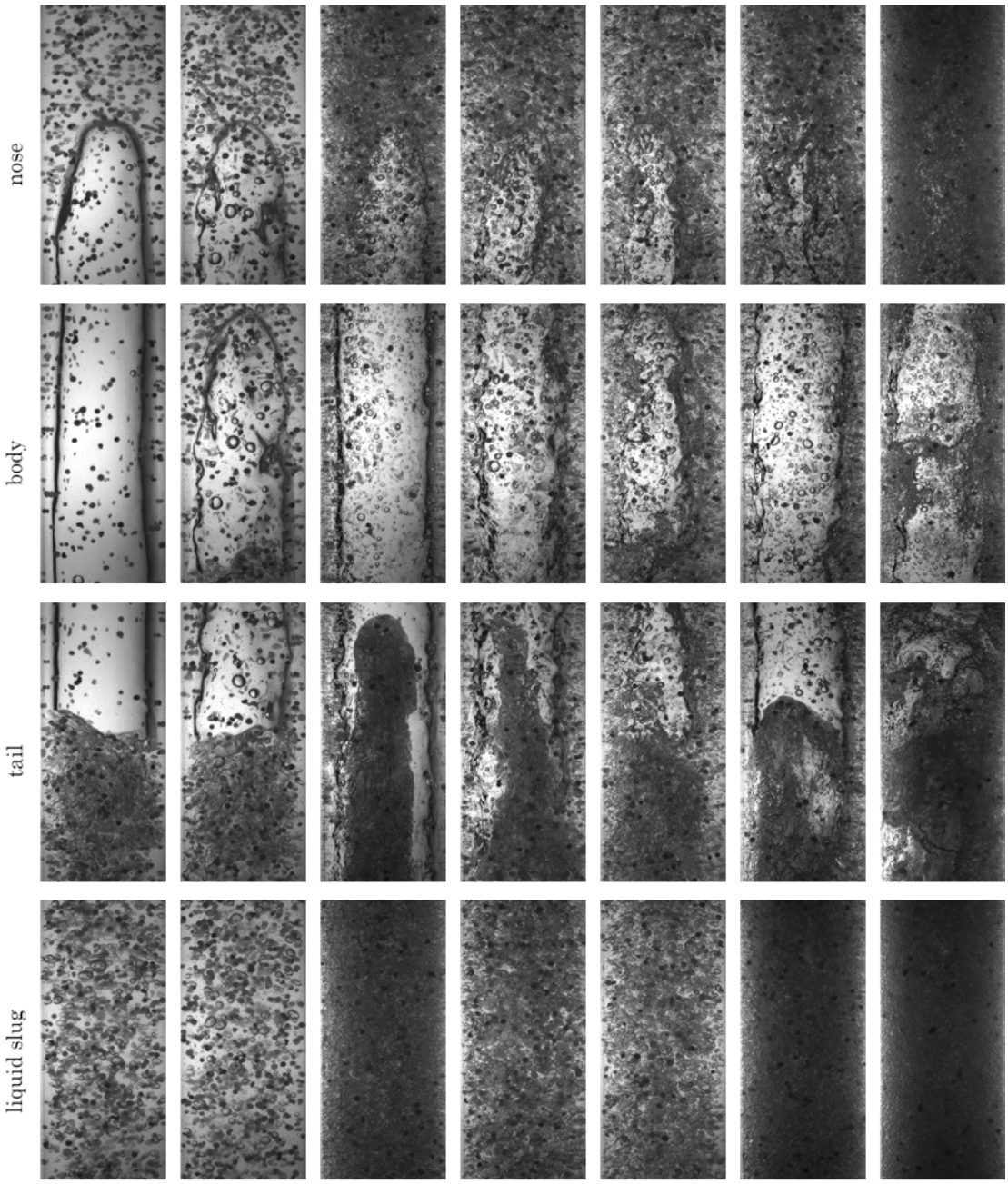

Fig. 10. Images of different elongated bubbles for a 5% of solid concentration three-phase flow at different Froude numbers.

However, these interactions may depend on the particle size (Douek et al., 1997; Chen and Fan, 1990). Furthermore, a further increase in Fr_m results in an increase in oscillations in the body and tail of the Taylor bubble.

3.6. Assessment of existing models and the proposed model

The predictions of the developed correlation and the exiting models presented in Tables 1 and 2 were evaluated with two different statistical parameters: APD and AAPD. The results for the APD parameter are summarized in Table 5. A positive APD indicates an overprediction while a negative value indicates an underprediction. The developed correlation shows a satisfactory performance for the several databases. Specifically, it shows the lowest APD (−1.64%) for the data of Shibata et al. (2023) for the measurements with 2.7 m pipe length.

In general, most models have worse predictions for measurements in the long pipe than for short pipe. The proposed correlation also gives a satisfactory result for the long-length pipe along with the model of Friedel (1979). Based on the values of APD, all the models under-predicted the data of Abdulkadir, in which the proposed correlation obtained the third-best value of APD (−78.15%). The evaluation of the models based on the absolute average percentage difference (AAPD) is summarized in Table 6. In general, the values of AAPD obtained with the proposed models are close to the APD values. This confirms the trends of overestimation or underestimation, as indicated by positive or negative APD values.

In the cases of the data of Tang et al. (2013), the lowest value of APD (0.99%) was obtained by the model of Shadloo et al. (2020). However, a high value of AAPD (489.45%) was obtained from this correlation, indicating a balance between highly overestimated and underestimated

Table 5
Assessment of existing models and the proposed model with the data of the literature: APD.

	APD(%)										
	Present study	Abdulkadir et al. (2021)	Aggour (1978)	Lu et al. (2018)	Saidj et al. (2018)	Shibata et al. (2023)-2.7 m	Shibata et al. (2023)-25 m	Sujumnong (1997)-G1	Sujumnong (1997)-G2	Sujumnong (1997)-Water	Tang et al. (2013)
McAdams (1949)	−47.87	−91.88	57.52	−8.56	−50.97	−36.21	−55.67	−8.09	−20.99	6.12	81.48
Cicchitti et al. (1960)	−46.86	−90.67	69.20	−8.27	−50.17	−35.39	−54.47	189.57	3612.29	37.96	109.40
Dukler et al. (1964)	−54.15	−92.69	32.63	−11.69	−56.42	−43.39	−63.10	−15.17	27.47	−14.01	28.66
Beattie and Whalley (1982)	−46.88	−90.98	54.02	−5.82	−49.34	−33.77	−55.67	7.96	163.29	−1.51	63.12
Fourar and Bories (1995)	−51.93	−92.45	40.64	−9.79	−54.28	−40.81	−60.87	−10.50	35.00	−7.05	43.15
Chisholm (1967)	−48.96	−91.94	47.93	−7.84	−53.62	−37.20	−58.73	**−2.51**	143.01	**−0.50**	57.61
Chisholm (1973)	−44.08	−89.19	72.18	−2.44	−39.93	−30.12	−52.55	23.50	2534	47.81	118.48
Mandhane et al. (1977)	−98.04	−99.65	−90.54	−98.91	−97.61	−97.82	−97.78	−89.52	−86.42	−83.39	−81.44
Müller-Steinhagen and Heck (1986)	−48.37	−92.86	56.78	−8.38	−52.55	−35.96	−55.09	−9.03	44.10	16.11	71.48
Mishima and Hibiki (1996)	−46.42	−91.37	58.58	−4.23	−43.88	−35.72	−57.47	19.46	244.99	11.18	77.61
Hwang and Kim (2006)	29.63	−77.70	124.94	101.25	**2.05**	199.77	193.13	63.46	83.81	52.00	117.22
Zhang et al. (2010)	−46.44	−91.37	55.97	−4.23	−43.89	−35.72	−57.47	21.23	250.75	9.03	73.95
Wilson et al. (2003)	−96.01	−99.27	−75.12	−98.52	−97.13	−95.81	−94.91	28.74	1211	−47.14	−47.28
Friedel (1979)	**−18.49**	−86.64	121.04	22.55	−11.17	3.99	**-29.84**	94.95	1343	53.84	201.94
Shannak (2008)	−46.56	−90.72	65.86	−8.19	−49.88	−35.15	−54.13	26.36	330.83	13.27	103.07
Awad and Muzychka (2008) [def. 1]	−51.34	−91.78	53.95	−15.39	−54.96	−40.47	−58.07	111.77	2375	23.25	87.12
Awad and Muzychka (2008) [def. 2]	−47.23	−91.28	62.98	−8.37	−50.48	−35.68	−54.91	5.94	**14.13**	15.06	94.93
Awad and Muzychka (2008) [def. 3]	−49.16	−91.53	58.91	−11.64	−52.58	−37.92	−56.39	56.05	1183	20.47	91.47
Lu et al. (2018)	−41.72	−90.57	76.30	−0.57	−38.93	−29.82	−52.39	35.19	296.31	25.68	106.90
Shadloo et al. (2020)	−22.96	**−67.03**	−653.10	78.96	57.28	−7.77	−81.31	−1249	3411	−977.80	**0.99**
Wallis (2020)	−52.61	−92.49	33.22	−1.15	−49.98	−42.86	−67.01	−8.89	140.24	−13.58	13.12
Whalley (1996)	−37.22	−90.09	91.36	2.92	−33.92	−23.27	−46.77	55.94	373.46	38.14	132.59
Sun and Mishima (2008)	−59.43	−91.84	**20.18**	−15.09	−57.83	−52.09	−70.90	41.15	581.02	−16.65	15.14
Awad (2007)	−56.69	−93.16	21.31	−6.65	−54.36	−48.10	−70.59	−17.88	114.23	−22.19	−1.52
Saisorn and Wongwises (2008)	−55.66	−92.97	20.97	−6.84	−53.15	−46.39	−69.15	−24.60	111.21	−36.09	−2.70
Ryan et al. (2023)	−40.54	−90.38	80.23	**0.34**	−37.70	−28.34	−51.12	38.68	307.70	28.89	113.61
Maher et al. (2020)	−35.45	−88.21	109.84	9.41	−36.81	−22.71	−45.44	489.95	7327	107.17	183.55
Developed Correlation	−22.50	−78.15	82.36	20.99	30.78	**−1.64**	−36.23	31.28	300.21	29.04	187.49

values. Therefore, based on AAPD values, the model proposed in this study presented satisfactory performance. The positive performance of the homogeneous models emerges as they obtain good values for data with high viscosity of Sujumnong (1997). Finally, it is observed that some correlations perform well for some datasets but also perform poorly under different conditions, demonstrating the complexity of two-phase upward flows.

Fig. 11 presents the prediction of the developed correlation with the experimental data in Fig. 11(a) and the collected data in Fig. 11(b). Three other models are added to the comparison: the McAdams (1949) homogeneous model, the separate phase models from Chisholm (1967) and Friedel (1979). The developed correlation shows an adequate performance compared to the various correlations proposed in the literature. In contrast, some existing models as that by Hwang and Kim (2006), Shadloo et al. (2020), and Maher et al. (2020) demonstrate also a good performance in specific databases. This is understandable since there are a few correlations developed to specific conditions. The proposed model demonstrated consistent accuracy across multiple datasets. It is not the most accurate model for all the datasets, but it stands out for its robustness and potential utility in predicting a wide range of two-phase frictional pressure drop in vertical upward pipelines.

The constant C proposed by Lu et al. (2018) and Ryan et al. (2023) obtained relatively similar and good results because of the relatively small difference in the values of C. Consequently, the model proposed by Chisholm (1967) also presents a satisfactory performance and reaffirms the wide and general use of this model. The correlation of Friedel (1979) performed well among the separate approaches. This model obtained results similar to those of the new proposed correlation, as shown in Fig. 11(b). The homogeneous models proved to be stable, had good results, and also adequately predicted the database with the highest viscosity from Sujumnong (1997). The model of McAdams (1949) is one of the first and simplest models, and it achieved positive performance. Among the models suggested by Awad and Muzychka (2008), the second definition had the best results among the collected databases. The positive performance of these homogeneous models may indicate that an implementation of a term based on viscosity in the proposed correlation can help in elaborating a generalist model for upward two-phase flows. Such investigations should be carried out in future studies.

For the three-phase flow data, the liquid and solid phases were assumed to be one pseudo-slurry phase. As explained in Section 1, this assumption made it possible to predict the three-phase frictional pressure drop using two-phase correlations, including the proposed model and the existing correlation from Tables 1 and 2. In this way, the slurry density was calculated using Eq. (46) and the slurry viscosity with Eq. (45).

The same statistical parameters employed for evaluating the correlation for two-phase experimental and literature data were used to evaluate the frictional pressure drop predictions for three-phase flow cases. The results of these statistical parameters are summarized in Table 7. The proposed correlation obtained the best results for all solid concentrations for the AAPD statistical parameter. The model proposed by Friedel (1979) also obtained a good prediction for three-phase flow data with statistical parameters comparable to those of the proposed correlation. A comparison between the proposed model with the experimental data is shown in Fig. 12. As expected, similar tendencies observed on two-phase data were also shown for three-phase

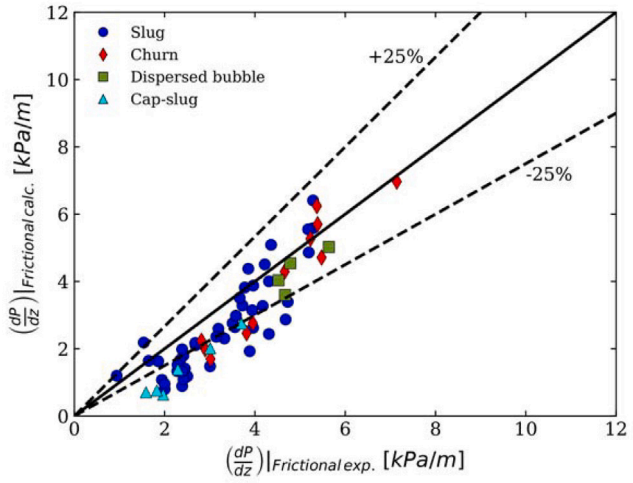

(a) Experimental two-phase flow data

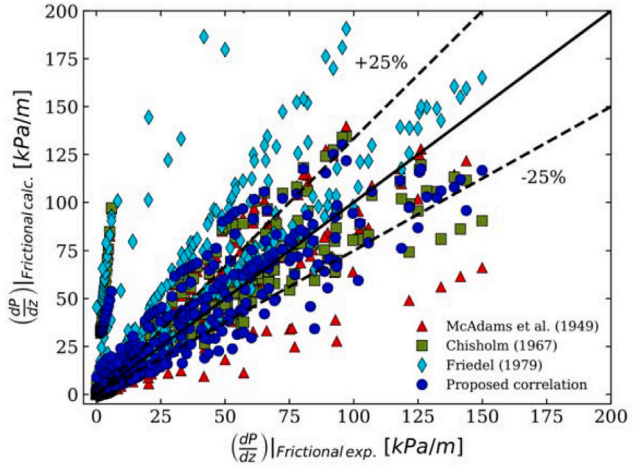

(b) Collected literature two-phase flow data from the studies summarized at Table 4

Fig. 11. Comparison between measured and calculated frictional pressure gradient.

flow cases. With the use of the slurry propriety, most of the correlations demonstrated satisfactory results, which proves that the assumption to consider gas–liquid–solid three-phase flow as gas-slurry flow can be successfully applied to three-phase flows with particles less dense than liquid.

4. Conclusion

The study presents a new database for pressure drop for gas–liquid and gas–liquid–solid with particles less dense than water, similar to hydrate particles that form during the production of gas and oil in offshore, for vertical upward pipelines. We conducted new experimental measurements on air–water two-phase and air–water–polypropylene three-phase flows in an experimental facility with an internal diameter of 30 mm.

Flow visualization using a high-speed camera was conducted to observe the Taylor bubble and dispersed bubbles in the liquid phase for different mixture Fr_m numbers. It is observed that an increase in Fr_m results in an increase in the oscillation at the Taylor bubble body and tail. Solid particles are dragged by the liquid toward the bubble nose and from the liquid film to the near wake region, where small dispersed bubbles are moved. The elongated bubble is highly distorted as we increase the Fr_m number.

The Froude number (Fr_m) influence in the Chisholm approach is also evaluated, and a new correlation is proposed for two-phase frictional pressure drop in vertical upward pipelines. The prediction of the proposed model and 27 frictional correlations were assessed against a collected dataset from the literature. The proposed model obtained satisfactory results with AAPD less than 30% for some databases that do not be used for its development. Thus, it showed the potential to be applied to a wide range of conditions in a two-phase vertical upward flow. The evaluation and comparison of the literature on frictional pressure drop correlations revealed that different phase properties, geometric parameters, and inlet parameters affect each correlation differently. Moreover, a comparison between two-phase and three different solid concentrations of total and frictional pressure drop data is performed and discussed. No visible impact of the presence of a solid less dense than the liquid phase is observed. Although it is too early to draw significant conclusions, further investigations with a wider range of mixture velocities might be performed to identify the possible effects on solids in two-phase flow. The Thomas slurry viscosity equation and the slurry density were used to adjust the parameters of the two-phase models and predict the gas–liquid–solid three-phase flow frictional pressure drop. This approach was evaluated and proved to produce satisfactory results. Indeed, both APD and AAPD statistical parameters were found lower than 30% for the three solid concentration cases studied.

The database helps in our comprehension of two-phase and three-phase flows in vertical upward pipelines. Further investigation will be performed to expand the range of flow parameters, phase properties, and solid concentration to advance our knowledge of two- and three-phase flows.

CRediT authorship contribution statement

Ronaldo Luís Höhn: Writing – review & editing, Visualization, Validation, Software, Methodology, Investigation, Conceptualization. **Abderraouf Arabi:** Writing – review & editing, Visualization, Validation, Software, Conceptualization. **Sylvana Verónica Varela Ballesta:** Writing – review & editing, Investigation. **Paolo Juan Sassi:** Writing – review & editing. **Jordi Pallarès:** Writing – review & editing, Funding acquisition. **Youssef Stiriba:** Writing – review & editing, Visualization, Software, Methodology, Funding acquisition, Conceptualization.

Declaration of competing interest

The authors declare that they have no known competing financial interests or personal relationships that could have appeared to influence the work reported in this paper.

Acknowledgments

This work was supported through the projects PID2020-113303GB-C21 and PID2023-146648NB-C21 funded by Ministerio de Ciencia e Innovación (MCIN) and Agencia Estatal de Investigación (AEI) and by project 2021SGR00732 from the Departament de Recerca i Universitats de la Generalitat de Catalunya as well as from the European Union's Horizon 2020 research and innovation programme under the Marie Skłodowska-Curie grant agreement No. 713679 and No. 945413, through the MartíFranquès COFUND Doctoral Programme. AA has received funding from the postdoctoral fellowships programme Beatriu de Pinós (2021 BP 00052), funded by the Secretary of Universities and Research (Government of Catalonia) and by the Horizon 2020 Programme of Research and Innovation of the European Union under the Marie Skłodowska-Curie grant agreement No. 801370.

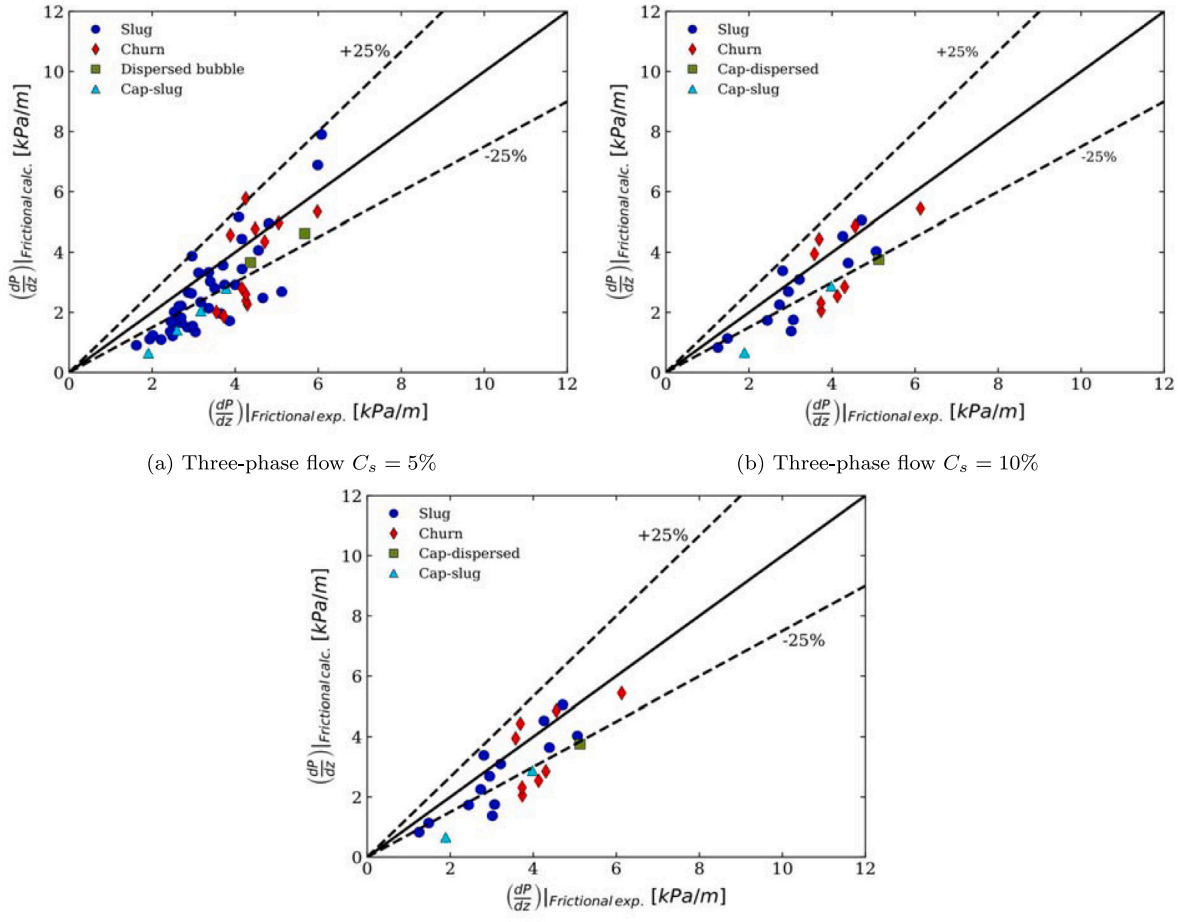

(a) Three-phase flow $C_s = 5\%$

(b) Three-phase flow $C_s = 10\%$

(c) Three-phase flow $C_s = 20\%$

Fig. 12. Comparison between measured and calculated frictional pressure gradient: Three-phase Flow.

Table 6
Assessment of existing models and the proposed model with the data of the literature: AAPD.

	AAPD (%)										
	Present study	Abdulkadir et al. (2021)	Aggour (1978)	Lu et al. (2018)	Saidj et al. (2018)	Shibata et al. (2023)-2.7 m	Shibata et al. (2023)-25 m	Sujumnong (1997)-G1	Sujumnong (1997)-G2	Sujumnong (1997)-Water	Tang et al. (2013)
McAdams (1949)	47.87	91.88	57.52	9.36	50.97	36.21	55.67	15.90	**58.06**	25.34	91.65
Cicchitti et al. (1960)	46.86	90.67	69.20	9.09	50.17	35.39	54.47	191.08	3612.67	46.26	118.30
Dukler et al. (1964)	54.15	92.69	36.25	12.20	56.42	43.39	63.10	21.36	76.95	27.91	61.06
Beattie and Whalley (1982)	46.88	90.98	54.44	7.26	49.34	33.77	55.67	15.65	181.35	24.11	76.55
Fourar and Bories (1995)	51.93	92.45	41.25	10.70	54.28	40.81	60.87	18.52	79.86	25.60	64.10
Chisholm (1967)	48.96	91.94	48.15	8.65	53.62	37.20	58.73	23.73	162.17	**22.28**	77.63
Chisholm (1973)	44.08	89.19	72.18	5.74	39.93	30.16	52.55	31.04	2554	55.35	125.78
Mandhane et al. (1977)	98.04	99.65	90.54	98.91	97.61	97.82	97.78	89.69	95.49	83.45	75.69
Müller-Steinhagen and Heck (1986)	48.37	92.86	56.78	9.21	52.55	35.96	55.09	19.83	85.94	27.52	84.12
Mishima and Hibiki (1996)	46.42	91.37	58.62	7.40	44.09	35.72	57.47	29.89	252.90	27.97	83.56
Hwang and Kim (2006)	61.11	77.70	124.94	101.25	31.69	199.77	193.13	67.14	100.47	52.62	120.25
Zhang et al. (2010)	46.44	91.37	56.06	7.40	44.10	35.72	57.47	30.39	258.36	27.88	80.77
Wilson et al. (2003)	96.01	99.27	80.59	98.52	97.13	95.81	94.91	171.45	1312	72.11	60.31
Friedel (1979)	27.91	86.64	121.04	22.55	**21.11**	11.60	**29.84**	95.36	1343	57.44	201.94
Shannak (2008)	46.56	90.72	65.86	9.01	49.88	35.15	54.13	32.11	345.60	28.67	111.68
Awad and Muzychka (2008) [def. 1]	51.34	91.78	53.95	15.39	54.96	40.47	58.07	121.26	2395	40.06	100.35
Awad and Muzychka (2008) [def. 2]	47.23	91.28	62.98	9.18	50.48	35.68	54.91	**13.80**	70.01	28.48	104.20
Awad and Muzychka (2008) [def. 3]	49.16	91.53	58.91	11.65	52.58	37.92	56.39	61.79	1204	33.33	102.54
Lu et al. (2018)	41.72	90.57	76.30	6.00	39.45	29.88	52.39	37.93	301.63	31.58	108.22
Shadloo et al. (2020)	34.41	**67.03**	784.57	88.55	64.65	21.35	81.31	1438	9322	1069	489.45
Wallis (2020)	52.61	92.49	50.09	9.85	50.23	42.86	67.01	31.35	157.59	32.23	60.87
Whalley (1996)	37.80	90.09	91.36	**5.65**	34.97	24.18	46.77	57.22	375.21	39.40	132.87
Sun and Mishima (2008)	59.43	91.84	**35.50**	15.68	57.83	52.09	70.90	43.78	581.02	31.95	**57.49**
Awad (2007)	56.69	93.16	45.85	11.26	54.36	48.10	70.59	33.00	138.48	35.21	60.77
Saisorn and Wongwises (2008)	55.66	92.97	48.88	10.63	53.15	46.39	69.15	34.58	140.02	47.34	66.80
Ryan et al. (2023)	40.63	90.38	80.23	5.81	38.32	28.60	51.12	40.72	312.46	33.15	114.45
Maher et al. (2020)	36.45	88.21	109.84	11.08	37.27	23.82	45.44	489.99	7327	107.71	185.47
Developed Correlation	**25.46**	78.15	86.97	20.99	36.46	**9.21**	36.23	45.69	311.13	57.31	188.90

Table 7
Three-phase gas–liquid–solid assessment of existing models and the proposed model with the data of the literature.

	APD (%)			AAPD (%)		
	5%	10%	20%	5%	10%	20%
McAdams (1949)	−48.23	−46.32	−36.18	48.27	46.32	37.82
Cicchitti et al. (1960)	−46.53	−44.29	−33.14	46.69	44.29	35.63
Dukler et al. (1964)	−54.87	−54.07	−46.39	54.87	54.07	46.39
Beattie and Whalley (1982)	−47.43	−45.90	−35.23	47.54	45.90	36.56
Fourar and Bories (1995)	−52.87	−51.75	−43.60	52.87	51.75	43.73
Chisholm (1967)	−49.49	−48.54	−39.86	49.49	48.54	40.53
Chisholm (1973)	−44.79	−43.46	−33.90	45.36	43.46	35.63
Mandhane et al. (1977)	−97.88	−97.61	−97.08	97.88	97.61	97.08
Müller-Steinhagen and Heck (1986)	−49.28	−48.15	−41.17	49.28	48.15	41.68
Mishima and Hibiki (1996)	−47.33	−45.98	−37.22	47.33	45.98	38.09
Hwang and Kim (2006)	28.13	26.86	27.84	62.73	57.59	58.77
Zhang et al. (2010)	−47.34	−45.99	−37.16	47.34	45.99	38.11
Wilson et al. (2003)	−95.53	−94.74	−93.54	95.53	94.74	93.54
Friedel (1979)	**−19.54**	**−18.50**	**−6.64**	32.44	29.74	29.15
Shannak (2008)	−46.59	−43.99	−32.53	46.80	43.99	35.05
Awad and Muzychka (2008) [def. 1]	−51.45	−49.19	−39.02	51.45	49.19	39.69
Awad and Muzychka (2008) [def. 2]	−47.39	−45.08	−34.37	47.50	45.08	36.09
Awad and Muzychka (2008) [def. 3]	−49.29	−47.02	−36.49	49.29	47.02	37.68
Lu et al. (2018)	−42.40	−40.73	−30.88	43.11	40.73	33.20
Shadloo et al. (2020)	−23.74	−19.41	6.48	32.16	35.85	38.08
Wallis (2020)	−54.53	−54.37	−47.83	54.53	54.37	47.83
Whalley (1996)	−37.80	−36.03	−25.44	40.13	36.33	30.40
Sun and Mishima (2008)	−60.25	−58.66	−49.10	60.25	58.66	49.10
Awad (2007)	−58.60	−58.50	−52.72	58.60	58.50	52.72
Saisorn and Wongwises (2008)	−57.49	−57.42	−51.29	57.49	57.42	51.29
Ryan et al. (2023)	−41.17	−39.42	−29.30	42.18	39.42	32.34
Maher et al. (2020)	−35.46	−32.19	−18.26	38.56	33.60	28.32
Developed Correlation	−23.43	−21.38	−8.66	**29.55**	**26.91**	**24.99**

References

Abdulkadir, M., Jatto, D., Abdulkareem, L., Zhao, D., 2020. Pressure drop, void fraction and flow pattern of vertical air–silicone oil flows using differential pressure transducer and advanced instrumentation. Chem. Eng. Res. Des. 159, 262–277. http://dx.doi.org/10.1016/j.cherd.2020.04.009.

Abdulkadir, M., Ugwoke, B., Abdulkareem, L., Zhao, D., Hernandez-Perez, V., 2021. Experimental investigation of the characteristics of the transition from spherical cap bubble to slug flow in a vertical pipe. Exp. Therm Fluid Sci. 124, 110349. http://dx.doi.org/10.1016/j.expthermflusci.2021.110349.

Aggour, M.A., 1978. Hydrodynamics and heat transfer in two-phase two-component flows (Ph.D. thesis). University of Winnipeg, Manitoba.

Al-Ruhaimani, F., Pereyra, E., Sarica, C., Al-Safran, E.M., Torres, C.F., 2016. Experimental analysis and model evaluation of high-liquid-viscosity two-phase upward vertical pipe flow. SPE J. 22 (03), 712–735. http://dx.doi.org/10.2118/184401-pa.

Arabi, A., Höhn, R.L., Pallares, J., Stiriba, Y., 2024. Practical aspects of multiphase slug frequency: An overview. Can. J. Chem. Eng. http://dx.doi.org/10.1002/cjce.25527.

Arabi, A., Saidj, F., Al-Sarkhi, A., Azzi, A., 2022. Analogy between vertical upward cap bubble and horizontal plug flow. SPE J. 27 (03), 1577–1596. http://dx.doi.org/10.2118/209235-pa.

Arabi, A., Salhi, Y., Zenati, Y., Si-Ahmed, E.-K., Legrand, J., 2021. A discussion on the relation between the intermittent flow sub-regimes and the frictional pressure drop. Int. J. Heat Mass Transfer 181, 121895. http://dx.doi.org/10.1016/j.ijheatmasstransfer.2021.121895.

Awad, M.M., 2007. Two-phase flow modeling in circular pipes (Ph.D. thesis). University of Newfoundland, Faculty of Engineering and Applied Science, Department of Mechanical Engineering.

Awad, M., Muzychka, Y., 2008. Effective property models for homogeneous two-phase flows. Exp. Therm Fluid Sci. 33 (1), 106–113. http://dx.doi.org/10.1016/j.expthermflusci.2008.07.006.

Beattie, D., Whalley, P., 1982. A simple two-phase frictional pressure drop calculation method. Int. J. Multiph. Flow 8 (1), 83–87. http://dx.doi.org/10.1016/0301-9322(82)90009-x.

Bouderbal, A., Salhi, Y., Arabi, A., Si-Ahmed, E.K., Legrand, J., Arhaliass, A., 2024. Experimental investigation of different sub-regimes in horizontal stratified and intermittent gas-liquid two-phase flow: Flow map and analysis of pressure drop fluctuations. Chem. Eng. Res. Des. 210, 407–427. http://dx.doi.org/10.1016/j.cherd.2024.08.029.

Cai, Q., D'Auria, F., Umminger, K., Bestion, D., Shan, J., 2022. Prioritizing pressure drop research in nuclear thermal hydraulics. Prog. Nucl. Energy 153, 104358. http://dx.doi.org/10.1016/j.pnucene.2022.104358.

Capovilla, M.S., Coutinho, R.P., de Sousa, P.C., Waltrich, P.J., 2019. Experimental investigation of upward vertical two-phase high-velocity flows in large-diameter pipes. Exp. Therm Fluid Sci. 102, 493–505. http://dx.doi.org/10.1016/j.expthermflusci.2018.12.024.

Cavalli, S., Alves, R.F., Bassi, C.L., Marcelino Neto, M.A., Sum, A.K., Morales, R.E.M., 2024. Modulation of slug flow characteristics observed in three-phase solid-liquid-gas flow measurements. Chem. Eng. Sci. 300, 120596. http://dx.doi.org/10.1016/j.ces.2024.120596.

Chen, Y.-M., Fan, L.-S., 1990. Drift flux in gas—liquid—solid fluidized systems from the dynamics of bed collapse. Chem. Eng. Sci. 45 (4), 935–945. http://dx.doi.org/10.1016/0009-2509(90)85016-7.

Chisholm, D., 1967. A theoretical basis for the lockhart-martinelli correlation for two-phase flow. Int. J. Heat Mass Transfer 10 (12), 1767–1778. http://dx.doi.org/10.1016/0017-9310(67)90047-6.

Chisholm, D., 1973. Pressure gradients due to friction during the flow of evaporating two-phase mixtures in smooth tubes and channels. Int. J. Heat Mass Transfer 16 (2), 347–358. http://dx.doi.org/10.1016/0017-9310(73)90063-x.

Cicchitti, A., Lombaradi, C., Silversti, M., G. Soldaini, R.Z., 1960. Two-phase cooling experiments– pressure drop heat transfer burnout measurements. Technical Report, Energia Nucleare.

Dang, Z., Yang, Z., Yang, X., Ishii, M., 2018. Experimental study of vertical and horizontal two-phase pipe flow through double 90 degree elbows. Int. J. Heat Mass Transfer 120, 861–869. http://dx.doi.org/10.1016/j.ijheatmasstransfer.2017.11.089.

Douek, R., Hewitt, G., Livingston, A., 1997. Hydrodynamics of vertical co-current gas-liquid-solid flows. Chem. Eng. Sci. 52 (23), 4357–4372. http://dx.doi.org/10.1016/s0009-2509(97)00182-6.

Dukler, A.E., Wicks, M., Cleveland, R.G., 1964. Frictional pressure drop in two-phase flow: A. a comparison of existing correlations for pressure loss and holdup. AIChE J. 10 (1), 38–43. http://dx.doi.org/10.1002/aic.690100117.

Fajemidupe, O.T., Aliyu, A.M., Baba, Y.D., Archibong-Eso, A., Yeung, H., 2019. Sand minimum transport conditions in gas–solid–liquid three-phase stratified flow in a horizontal pipe at low particle concentrations. Chem. Eng. Res. Des. 143, 114–126. http://dx.doi.org/10.1016/j.cherd.2019.01.014.

Fourar, M., Bories, S., 1995. Experimental study of air-water two-phase flow through a fracture (narrow channel). Int. J. Multiph. Flow 21 (4), 621–637. http://dx.doi.org/10.1016/0301-9322(95)00005-i.

Friedel, L., 1979. Improved friction pressure drop correlations for horizontal and vertical two-phase pipe flow. In: European Two-phase Group Meeting. Ispra, Italy, URL https://cir.nii.ac.jp/crid/1571417124944185600.

Ghajar, A.J., Bhagwat, S.M., 2014. Flow patterns, void fraction and pressure drop in gas-liquid two phase flow at different pipe orientations. In: Frontiers and Progress in Multiphase Flow I. Springer International Publishing, pp. 157–212. http://dx.doi.org/10.1007/978-3-319-04358-6_4.

Guazzelli, E., Pouliquen, O., 2018. Rheology of dense granular suspensions. J. Fluid Mech. 852, http://dx.doi.org/10.1017/jfm.2018.548.

Hatakeyama, N., Masuyama, T., 1995. Pressure drops in vertical gas-liquid-solid three-phase flow.. Shigen-to-Sozai 111 (7), 465–470. http://dx.doi.org/10.2473/shigentosozai.111.465.

Hatate, Y., Nomura, H., Fujita, T., Tajiri, S., Hidaka, N., Ikari, A., 1986. Gas holdup and pressure drop in three-phase vertical flows of gas-liquid-fine solid particles system.. J. Chem. Eng. Japan 19 (1), 56–61. http://dx.doi.org/10.1252/jcej.19.56.

Hewitt, G., 1985. Experimental and modelling studies of annular flow in the region between flow reversal and the pressure drop minimum. Physico-Chem. Hydrodyn. 6, 43–50, URL https://cir.nii.ac.jp/crid/1573950399582951808.

Hughmark, G., 1965. Holdup and heat transfer in horizontal slug gas-liquid flow. Chem. Eng. Sci. 20 (12), 1007–1010. http://dx.doi.org/10.1016/0009-2509(65)80101-4.

Hwang, Y.W., Kim, M.S., 2006. The pressure drop in microtubes and the correlation development. Int. J. Heat Mass Transfer 49 (11–12), 1804–1812. http://dx.doi.org/10.1016/j.ijheatmasstransfer.2005.10.040.

Jayanti, S., Hewitt, G., 1992. Prediction of the slug-to-churn flow transition in vertical two-phase flow. Int. J. Multiph. Flow 18 (6), 847–860. http://dx.doi.org/10.1016/0301-9322(92)90063-m.

Lockhart, W.R., Martinelli, R.C., 1949. Proposed correlation of data for isothermal two-phase, two-component flow in pipes. Chem. Eng. Prog. 45 (1), 39–48, URL https://cir.nii.ac.jp/crid/1574231874770760320.

Lu, C., Kong, R., Qiao, S., Larimer, J., Kim, S., Bajorek, S., Tien, K., Hoxie, C., 2018. Frictional pressure drop analysis for horizontal and vertical air-water two-phase flows in different pipe sizes. Nucl. Eng. Des. 332, 147–161. http://dx.doi.org/10.1016/j.nucengdes.2018.03.036.

Maher, D., Hana, A., Habib, S., 2020. New correlations for two phase flow pressure drop in homogeneous flows model. Therm. Eng. 67 (2), 92–105. http://dx.doi.org/10.1134/s0040601520020032.

Maldonado, P.A.D., Gmyterco, A., Rodrigues, C.C., Mancilla, E., dos Santos, E.N., da Silva, M.J., da Fonseca Junior, R., Morales, R.E., 2023. Experimental characterization of the dispersed bubbles in the slug of an air–water slug flow in a vertical pipe. J. Brazilian S. Mech. Sci. Eng. 45 (9), http://dx.doi.org/10.1007/s40430-023-04360-1.

Maldonado, P., Rodrigues, C.C., Mancilla, E., dos Santos, E.N., da Fonseca Junior, R., M. Neto, M.A., da Silva, M.J., E. M. Morales, R., 2024. Spatial distribution of void fraction in the liquid slug in vertical gas-liquid slug flow. Exp. Therm Fluid Sci. 151, 111093. http://dx.doi.org/10.1016/j.expthermflusci.2023.111093.

Mandhane, J., Gregory, G., Aziz, K., 1977. Critical evaluation of friction pressure-drop prediction methods for gas-liquid flow in horizontal pipes. J. Pet. Technol. 29 (10), 1348–1358. http://dx.doi.org/10.2118/6036-pa.

McAdams, W.H., 1949. Vaporization inside horizontal tubes-II benzene-oil mixtures. Trans. ASME 39, 39–48, URL https://cir.nii.ac.jp/crid/1570009750060630016.

Mishima, K., Hibiki, T., 1996. Some characteristics of air-water two-phase flow in small diameter vertical tubes. Int. J. Multiph. Flow 22 (4), 703–712. http://dx.doi.org/10.1016/0301-9322(96)00010-9.

Mueller, S., Llewellin, E.W., Mader, H.M., 2009. The rheology of suspensions of solid particles. Proc. Royal Soc. A: Mathe. Phys. Eng. Sci. 466 (2116), 1201–1228. http://dx.doi.org/10.1098/rspa.2009.0445.

Müller-Steinhagen, H., Heck, K., 1986. A simple friction pressure drop correlation for two-phase flow in pipes. Chem. Eng. Process. Process Intensif. 20 (6), 297–308. http://dx.doi.org/10.1016/0255-2701(86)80008-3.

Muzychka, Y.S., Awad, M.M., 2010. Asymptotic generalizations of the lockhart–martinelli method for two phase flows. J. Fluids Eng. 132 (3), http://dx.doi.org/10.1115/1.4001157.

Owen, D.J., 1986. An experimental and theoretical analysis of equilibrium annular flow (Ph. D. thesis). University of Birmingham, England, URL https://cir.nii.ac.jp/crid/1570009749909001984.

Passoni, S., Carraretto, I.M., Mereu, R., Colombo, L.P.M., 2023. Two-phase stratified flow in horizontal pipes: A CFD study to improve prediction of pressure gradient and void fraction. Chem. Eng. Res. Des. 191, 38–49. http://dx.doi.org/10.1016/j.cherd.2023.01.016.

Rahman, M., Adane, K.F., Sanders, R.S., 2013. An improved method for applying the lockhart–martinelli correlation to three-phase gas–liquid–solid horizontal pipeline flows. Can. J. Chem. Eng. 91 (8), 1372–1382. http://dx.doi.org/10.1002/cjce.21843.

Rosas, L.M.M., Bassani, C.L., Alves, R.F., Schneider, F.A., Neto, M.A.M., Morales, R.E.M., Sum, A.K., 2018. Measurements of horizontal three-phase solid-liquid-gas slug flow: Influence of hydrate-like particles on hydrodynamics. AIChE J. 64 (7), 2864–2880. http://dx.doi.org/10.1002/aic.16148.

Ryan, D., Kong, R., Kang, D., Dix, A., Kim, S., Bian, J., 2023. Effects of pipe inclination on global two-phase flow parameters. Nucl. Technol. 209 (10), 1485–1494. http://dx.doi.org/10.1080/00295450.2022.2160172.

Sadatomi, M., Sato, Y., Yoshinaga, T., Inagaki, K., 1990. Hydraulic lifting of coarse particles in vertical pipes. Japanese J. Multiphase Flow 4 (2), 111–124. http://dx.doi.org/10.3811/jjmf.4.111.

Saidj, F., Hasan, A., Bouyahiaoui, H., Zeghloul, A., Azzi, A., 2018. Experimental study of the characteristics of an upward two-phase slug flow in a vertical pipe. Prog. Nucl. Energy 108, 428–437. http://dx.doi.org/10.1016/j.pnucene.2018.07.001.

Saisorn, S., Wongwises, S., 2008. Flow pattern, void fraction and pressure drop of two-phase air–water flow in a horizontal circular micro-channel. Exp. Therm Fluid Sci. 32 (3), 748–760. http://dx.doi.org/10.1016/j.expthermflusci.2007.09.005.

Sakaguchi, T., Minagawa, H., Tomiyama, A., Shakutsui, H., 1993. Pressure drop in gas-liquid-solid three-phase slug flow in vertical pipes. Exp. Therm Fluid Sci. 7 (1), 49–60. http://dx.doi.org/10.1016/0894-1777(93)90080-3.

Sassi, P., Fernández, G., Stiriba, Y., Pallarès, J., 2022. Effect of solid particles on the slug frequency, bubble velocity and bubble length of intermittent gas–liquid two-phase flows in horizontal pipelines. Int. J. Multiph. Flow 149, 103985. http://dx.doi.org/10.1016/j.ijmultiphaseflow.2022.103985.

Sassi, P., Pallarès, J., Stiriba, Y., 2020a. Visualization and measurement of two-phase flows in horizontal pipelines. Exper. Comput. Multiphase Flow 2 (1), 41–51. http://dx.doi.org/10.1007/s42757-019-0022-1.

Sassi, P., Stiriba, Y., Lobera, J., Palero, V., Pallarès, J., 2020b. Experimental analysis of gas–liquid–solid three-phase flows in horizontal pipelines. Flow Turbul. Combust. 105 (4), 1035–1054. http://dx.doi.org/10.1007/s10494-020-00141-1.

Sawai, T., Kaji, M., Kasugai, T., Nakashima, H., Mori, T., 2004. Gas–liquid interfacial structure and pressure drop characteristics of churn flow. Exp. Therm Fluid Sci. 28 (6), 597–606. http://dx.doi.org/10.1016/j.expthermflusci.2003.09.003.

Shadloo, M.S., Rahmat, A., Karimipour, A., Wongwises, S., 2020. Estimation of pressure drop of two-phase flow in horizontal long pipes using artificial neural networks. J. Energy Resour. Technol. 142 (11), http://dx.doi.org/10.1115/1.4047593.

Shannak, B.A., 2008. Frictional pressure drop of gas liquid two-phase flow in pipes. Nucl. Eng. Des. 238 (12), 3277–3284. http://dx.doi.org/10.1016/j.nucengdes.2008.08.015.

Shibata, N., Miwa, S., Sawa, K., Moriya, H., Takahashi, M., Murayama, T., Tenma, N., 2023. The void fraction and frictional pressure drop of upward two-phase flow under high pressure brine condition. Chem. Eng. Sci. 268, 118399. http://dx.doi.org/10.1016/j.ces.2022.118399.

Shoham, O., 2006. Mechanistic modeling of gas-liquid two-phase flow in pipes. Society of Petroleum Engineers, Richardson, TX.

Sujumnong, M., 1997. Heat transfer, pressure drop and void fraction in two-phase, two-component flow in a vertical tube (Ph.D. thesis). Department of Mechanical and Industrial Engineering, University of Manitoba.

Sun, L., Mishima, K., 2008. Evaluation analysis of prediction methods for two-phase flow pressure drop in mini-channels. In: Volume 2: Fuel Cycle and High Level Waste Management; Computational Fluid Dynamics, Neutronics Methods and Coupled Codes; Student Paper Competition. In: ICONE16, ASMEDC, http://dx.doi.org/10.1115/icone16-48210.

Takano, S., Masanobu, S., Kanada, S., Ono, M., 2021. Experimental study on void fractions and pressure drops in three-phase flow for deep sea mining. In: Volume 5: Ocean Space Utilization. In: OMAE2021, American Society of Mechanical Engineers, http://dx.doi.org/10.1115/omae2021-60472.

Takano, S., Masanobu, S., Kanada, S., Ono, M., 2023. Correlation for calculating frictional pressure drops in vertical three-phase flows for subsea-resource production. Ocean Eng. 275, 114121. http://dx.doi.org/10.1016/j.oceaneng.2023.114121.

Takano, S., Masanobu, S., Yamamoto, J., Kanada, S., Ono, M., Sasagawa, H., 2020. Experimental study on three phase flow in inclined pipe for deep sea mining. In: Volume 5: Ocean Space Utilization. In: OMAE2020, American Society of Mechanical Engineers, http://dx.doi.org/10.1115/omae2020-18257.

Tang, C.C., Tiwari, S., Ghajar, A.J., 2013. Effect of void fraction on pressure drop in upward vertical two-phase gas-liquid pipe flow. J. Eng. Gas Turbines Power 135 (2), http://dx.doi.org/10.1115/1.4007762.

Tarahomi, M.A., Emamzadeh, M., Ameri, M., 2023. Scaling two-phase gas-liquid flow in horizontal pipes. Chem. Eng. Res. Des. 200, 592–601. http://dx.doi.org/10.1016/j.cherd.2023.11.029.

Thomas, D.G., 1965. Transport characteristics of suspension: VIII. A note on the viscosity of Newtonian suspensions of uniform spherical particles. J. Colloid Sci. 20 (3), 267–277. http://dx.doi.org/10.1016/0095-8522(65)90016-4.

Wallis, G.B., 2020. One-dimensional two-phase flow. In: Dover books on engineering, Dover Publications, Inc, Mineola, New York.

Whalley, P.B., 1996. Two-phase flow and heat transfer. In: Oxford science publications, Oxford University Press, Oxford [u.a.].

Wilson, M., Newell, T., Chato, J., Infante Ferreira, C., 2003. Refrigerant charge, pressure drop, and condensation heat transfer in flattened tubes. Int. J. Refrig. 26 (4), 442–451. http://dx.doi.org/10.1016/s0140-7007(02)00157-3.

Zhang, W., Hibiki, T., Mishima, K., 2010. Correlations of two-phase frictional pressure drop and void fraction in mini-channel. Int. J. Heat Mass Transfer 53 (1–3), 453–465. http://dx.doi.org/10.1016/j.ijheatmasstransfer.2009.09.011.

Zhang, D., Liu, S., Zhang, J., Hou, L.-t., Xu, J.-y., 2020. Experimental investigation of the flow characteristics in crude oil containing sand and gas flowing along vertical pipelines. ACS Omega 5 (48), 31262–31271. http://dx.doi.org/10.1021/acsomega.0c04637.

Zhang, H., Umehara, Y., Yoshida, H., Mori, S., 2024. Prediction of interfacial shear stress and pressure drop in vertical two-phase annular flow. Int. J. Heat Mass Transfer 218, 124750. http://dx.doi.org/10.1016/j.ijheatmasstransfer.2023.124750.